

### 3. RESULTS

#### I 12-LIPOXYGENASE PATHWAY IN PLATELETS AND OTHER CELLS

##### 3.1 DETECTION OF PHGPx AND DETERMINATION OF ITS ACTIVITY

To detect PHGPx in human platelets, several experimental strategies were used.

##### 3.1.1 Detection by Western Blotting

Western blotting was performed using two different antibodies (i) a rabbit polyclonal antibody raised against a 15 amino acid fragment of human PHGPx (Fig. 1a), and (ii) a polyclonal antibody against porcine PHGPx (Fig. 1b). Lysate from A431 cells and red blood cells (RBC) were also examined as positive and negative controls respectively.

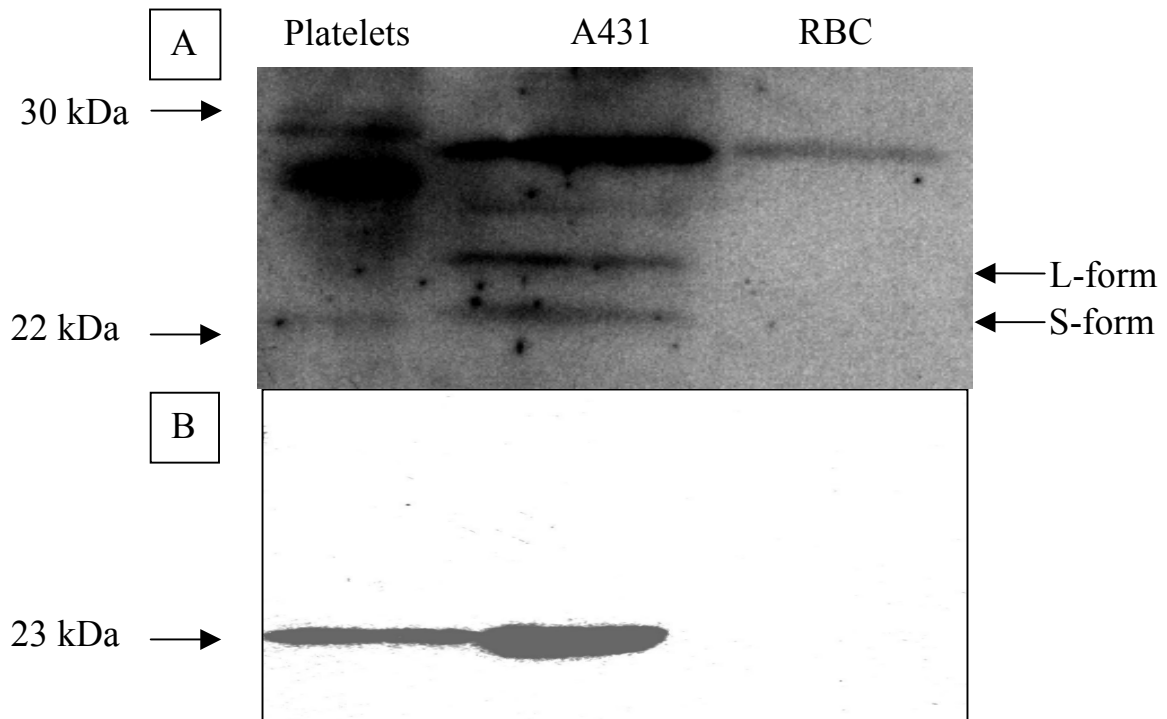


Figure 1. Western blot against human PHGPx showing the occurrence of PHGPx in human platelets. Lysate was prepared as described in Materials and Methods and Western blotting was performed with a rabbit polyclonal antibody raised against a 15 amino acid fragment of human PHGPx (A) and a polyclonal antibody against porcine PHGPx (B). A431 and red blood cell (RBC) lysates were used as positive and negative controls, respectively.

The antibody raised against a 15 amino acid fragment yielded a band at ~ 23 kDa, corresponding to the molecular weight of PHGPx, in human platelet lysate. In A431 cell lysate, two bands were observed corresponding to approximate MW of 23 and 25 kDa. The two bands may correspond to the short (S)- and long (L)-forms. The L-form occurs in

mitochondria which are absent in platelets. The antibody against porcine PHGPx yielded a single band at ~ 23 kDa in both platelet and A431 lysate. The RBC lysate tested negative with both antibodies.

### 3.1.2 Detection by PCR

Total RNA was isolated from human bone marrow megakaryocytes, human platelets and A431 cells. Reverse transcription was carried out with 5 µg RNA, followed by PCR using specific primers for PHGPx and 12-LOX (Fig. 2). A positive reaction for 12-LOX with all three cell types was obtained. A PHGPx product was detected only in megakaryocytes and A431 cells.

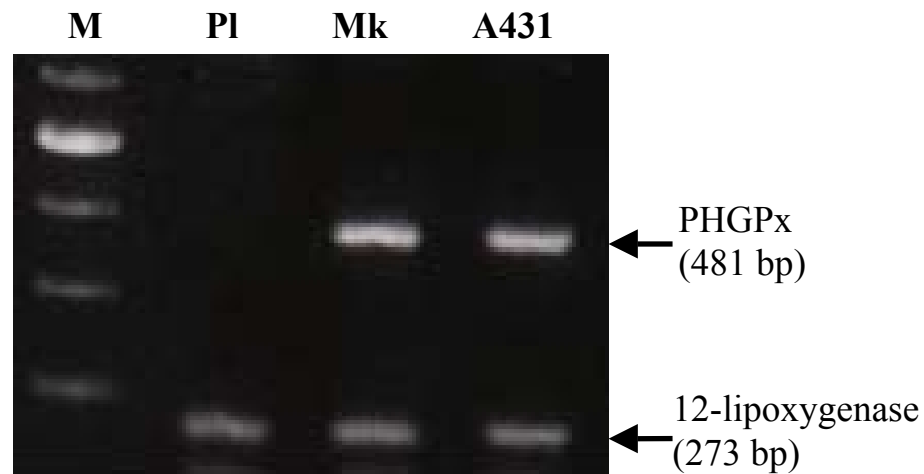


Figure 2. RT-PCR detection of the mRNA for PHGPx and 12-LOX in human platelets (Pl), megakaryocytes (Mk) and A431 cells. The PCR products were separated on a 2% agarose gel. (M = Marker).

The mRNA from human platelets was extracted using oligo-dT cellulose columns and RT-PCR performed for the detection of PHGPx mRNA. Traces of PHGPx mRNA were detected in platelets as compared to large amounts in human bone marrow megakaryocytes. The near absence of PHGPx mRNA in platelets is in contrast with the detection of protein. These results may be interpreted by the fact that the PHGPx mRNA has a short half-life as compared with 12-LOX mRNA.

### 3.1.2.1 OCCURRENCE OF SHORT-LIVED PHGPX-MRNA IN HUMAN MEGAKARYOCYTES

During megakaryopoiesis platelets lose their nucleus. To verify if the absence of PHGPx mRNA in platelets may be due to a shorter half-life of the PHGPx messenger as compared to other mRNAs, the breakdown rates of PHGPx messenger in the human megakaryoblast cell line UT-7 before and after differentiation by phorbol-12-myristate-13-acetate (PMA) were examined. The transcription was stopped by the addition of actinomycin D and the level of messenger was followed in dependence on time (Fig. 3).  $\beta$ -actin mRNA levels were used as control. The half-life of PHGPx mRNA in the non-differentiated and differentiated cells was found to be  $\sim 3$  h and 0.5 h respectively. Provided that the PMA model of megakaryoblast differentiation reflects the *in vivo* conditions in a correct manner, this observation affords a plausible explanation for the extremely low level of PHGPx mRNA in human platelets.

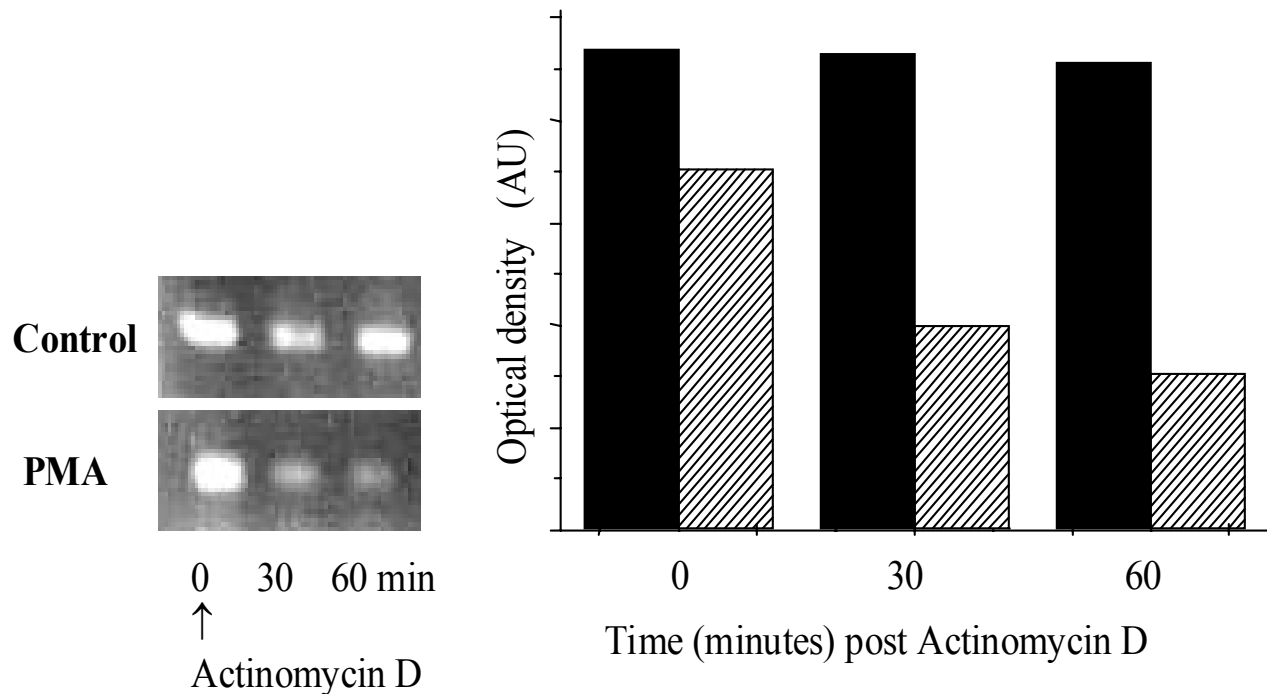


Figure 3. Rates of PHGPx mRNA breakdown in non-differentiated (control) and PMA differentiated UT-7 cells. The column pairs (right panel) represents the relative levels of PHGPx mRNA normalised for  $\beta$ -actin for the control cells (black columns) and PMA-treated cells (hatched columns).

### 3.1.3 PHGPx and GPx-1 Activity in human platelets

To detect specifically PHGPx activity in lysates of human platelets, a PHGPx-specific substrate, 1-palmitoyl-2-[15-hydroperoxy-5Z,8Z,11Z,13E-eicosatetraenoyl]-phosphatidylcholine (PAPC -OOH), was applied in a coupled spectrophotometric assay with glutathione

reductase. This substrate does not react with cytosolic GPx-1. The PAPC-OOH was prepared as described in Materials and Methods. Briefly, 1 mg of soybean lipoxygenase was added to 780  $\mu\text{g}$  PAPC, extracted and purified by reverse-phase HPLC (Nucleosil 1005 C<sub>8</sub> column). Enzyme activity in A431 cell lysate was used as positive control (Fig. 4a). A dose-dependent activity was observed with platelet cytosol when different quantities of platelet protein were incubated with PAPC-OOH (Fig. 4b).

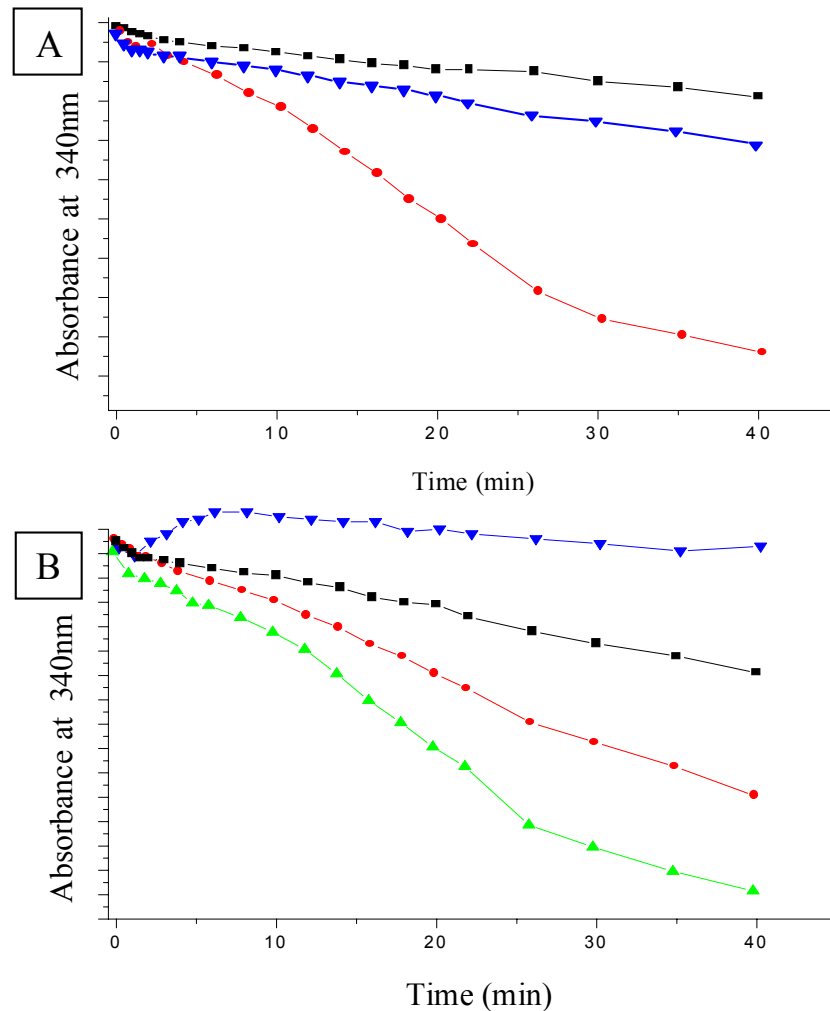


Figure 4. PHGPx activity in A431 cell cytosol fraction (A) (Blank ■, 50  $\mu\text{l}$  lysate ● and 50  $\mu\text{l}$  lysate + 2 mM iodoacetate ▼) and human platelet cytosol fraction (B) (0.1 mg protein ■, 0.25 mg protein ●, 0.5 mg protein ▲ and 0.5 mg protein + 2 mM iodoacetate ▼) incubated with 20  $\mu\text{M}$  PAPC-OOH as substrate.

This activity was completely blocked by 2 mM iodoacetate, an inhibitor of selenoenzymes i.e. GPx-1 and PHGPx, in both A431 lysate and platelet cytosol (Fig. 4a and b respectively). Inasmuch as GPx-1 does not react with PAPC-OOH, the inhibitory effect of iodoacetate must be ascribed to its interaction with PHGPx. Moreover, the strong inhibition by iodoacetate

appears to rule out the participation of enzymes other than PHGPx, such as non-selenium glutathione peroxidases and glutathione transferases, in the PAPC-OOH reductase activity of platelet and A431 cytosol.

The particulate fraction from both human platelets and A431 cells were also tested for PHGPx activity. The platelet particulate fraction exhibited ~ 10% of the activity as compared to the cytosol fraction. In A431 cells, however, approximately 45% of the total activity was found to reside in the particulate fraction containing the mitochondria.

For comparison, GPx-1 activity was measured with H<sub>2</sub>O<sub>2</sub> as substrate. A dose-dependent GPx-1 activity was observed (Fig. 5). The activity measured with a GPx-1 specific substrate, *tert*-butylhydroperoxide, was ~ 2× lower than with H<sub>2</sub>O<sub>2</sub>.

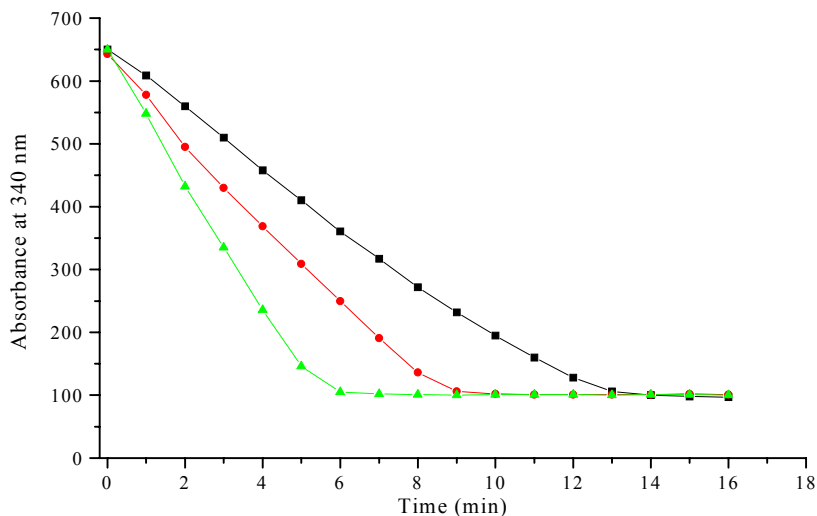


Figure 5. GPx-1 activity in human platelet cytosol using H<sub>2</sub>O<sub>2</sub> as substrate. 0.027 mg protein ■, 0.054 mg protein ● and 0.108 mg protein ▲ were incubated with 25 mM H<sub>2</sub>O<sub>2</sub> and the activity was measured spectrophotometrically at 340 nm.

In Table 1 activities of GPx-1 and PHGPx measured in human platelets, A431 cells, the human acute myeloid leukemia cell line UT-7 and the rat  $\beta$ -islet cell line RINm5F are compiled. The three cell types human platelets, A431 and UT-7 did not differ significantly with respect to the total activities of GPx-1 and PHGPx. In RINm5F cells no GPx-1 activity was detectable. The PHGPx activity in RINm5F cells was found to be ~ 2× higher as compared to the other cells.

Table 1. PHGPx and GPx-1 activity in human platelets, A431, UT-7 and RINm5F cells. Activity was measured with 20  $\mu$ M PAPC-OOH and 0.25 mM H<sub>2</sub>O<sub>2</sub> as substrate respectively. Number of experiments is indicated in parenthesis.

Activity (nkat/mg protein)	Platelets	A431	UT-7	RINm5F
PHGPx	1.4 $\pm$ 0.2 (4)	1.0 $\pm$ 0.04 (3)	1.2 (2)	2.4 (2)
GPx-1	68.4 (2)	72.5 (2)	63.4 $\pm$ 4.4 (5)	nd (2)

nd = not detectable

### **3.2 MEASUREMENT OF ARACHIDONIC ACID AND THE 12-LOX METABOLITES 12-HpETE, 12-HETE AND HEPOXILINS**

#### **3.2.1 Optimisation of the Extraction**

Initial experiments extracted according to Bryant *et al.* (1982), using the extraction buffer ether/methanol/1M citric acid (135:15:1, v/v/v), and analysed by HPLC exhibited both poor recovery and reproducibility. In order to investigate the reason for poor extraction, the effect of pH on the extraction and product profile was examined (Table 2). The pH of the samples was adjusted before extraction using 1 M citric acid or an equivalent volume of 1 M sodium citrate. The 12-LOX metabolites were analysed by HPLC as described in Materials and Methods. The total recovery of the metabolites AA, 12-HpETE, 12-HETE and 12-HHTrE was  $\sim 2\times$  higher at pH 7.5 than at pH less than 2.5. At neutral pH, the ratio of 12-HETE:12-HpETE was found to be approximately 1:1.36. The ratio of 12-HETE:12-HpETE in the acidified sample (<pH 2.5) was 1:0.9. All further extractions were performed without prior acidification using the extraction buffer ether/methanol/1 M sodium citrate (135:15:1, v/v/v). The pH effect may be explained by the difference in the solvent systems. Ether/methanol/sodium citrate is a homogenous solvent mixture as compared to the two phase-system of water-ethylacetate in which acidification is required. An acidic medium, however, enhances the risk of acid-catalysed decomposition of 12-HpETE.

Table 2. Effect of pH on the extraction of 12-lipoxygenase metabolites from washed human platelets ( $3.2 \times 10^8$  cells/ml) treated with 130  $\mu$ M arachidonic acid. Samples were extracted and analysed by HPLC (Straight phase Supelcosil LC-S1 column (250 x 46 mm; 5  $\mu$ m particle size), solvent system : n-hexane:i-propanol:acetic acid (100:2:1, v/v/v), flow rate 1 ml/min).

Metabolite (nmoles)	pH 7.5	pH 4.0	pH 3.0	<pH 2.5
Arachidonic acid	32.5	18.32	17.99	16.76
12-HETE	3.69	2.83	2.42	2.89
12-HpETE	5.02	3.18	2.62	2.62
12-HHTrE	0.35	0.67	0.69	0.42
TOTAL	41.56	25	23.72	22.69

### 3.2.2 Identification of the end products by HPLC and quantification

HPLC analysis of the authentic standards AA, 12-HpETE, 12-HETE and 12-HHTrE with respect to their respective retention time and UV-spectra was performed as described under Material and Methods. Figure 6 shows the typical retention times and UV-spectra of AA and 12-LOX metabolites. Arachidonic acid exhibits an absorption maximum at 196 nm. The eluent system [n-hexane:i-propanol:acetic acid (100:2:1, v/v/v)] does not allow detection at this wavelength (cut off = 200 nm). Authentic standard of AA exhibited an absorption at 208 nm, therefore this wavelength was used for detection and quantification of AA.

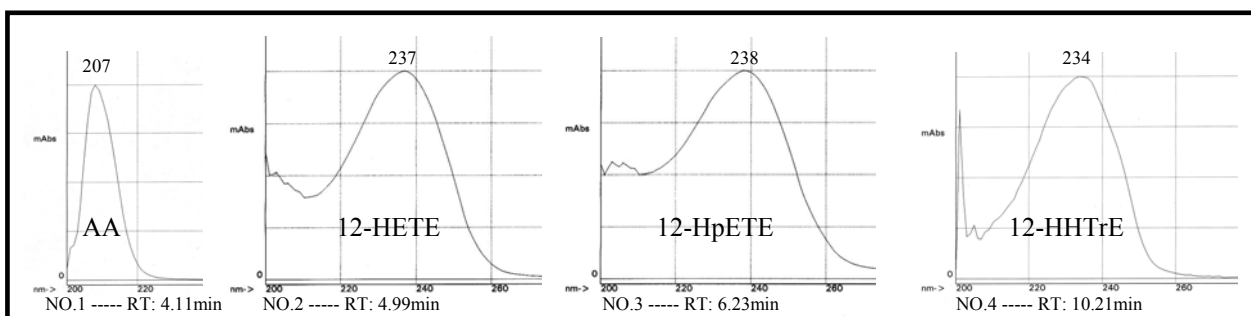


Figure 6. Typical UV-spectra and retention times (RT) of the authentic standards AA, 12-HETE, 12-HpETE and 12-HHTrE. (Straight phase Supelcosil LC-S1 column (250 x 46 mm; 5  $\mu$ m particle size), solvent system : n-hexane:i-propanol:acetic acid (100:2:1, v/v/v), flow rate 1 ml/min).

The authentic standards of AA and 12-HETE were used to plot calibration curves for quantification (Fig. 7a and b). The calibration curve plotted for 12-HETE was used for the quantification of 12-HpETE as they exhibit the same  $\lambda_{\max}$  and  $\epsilon$ .

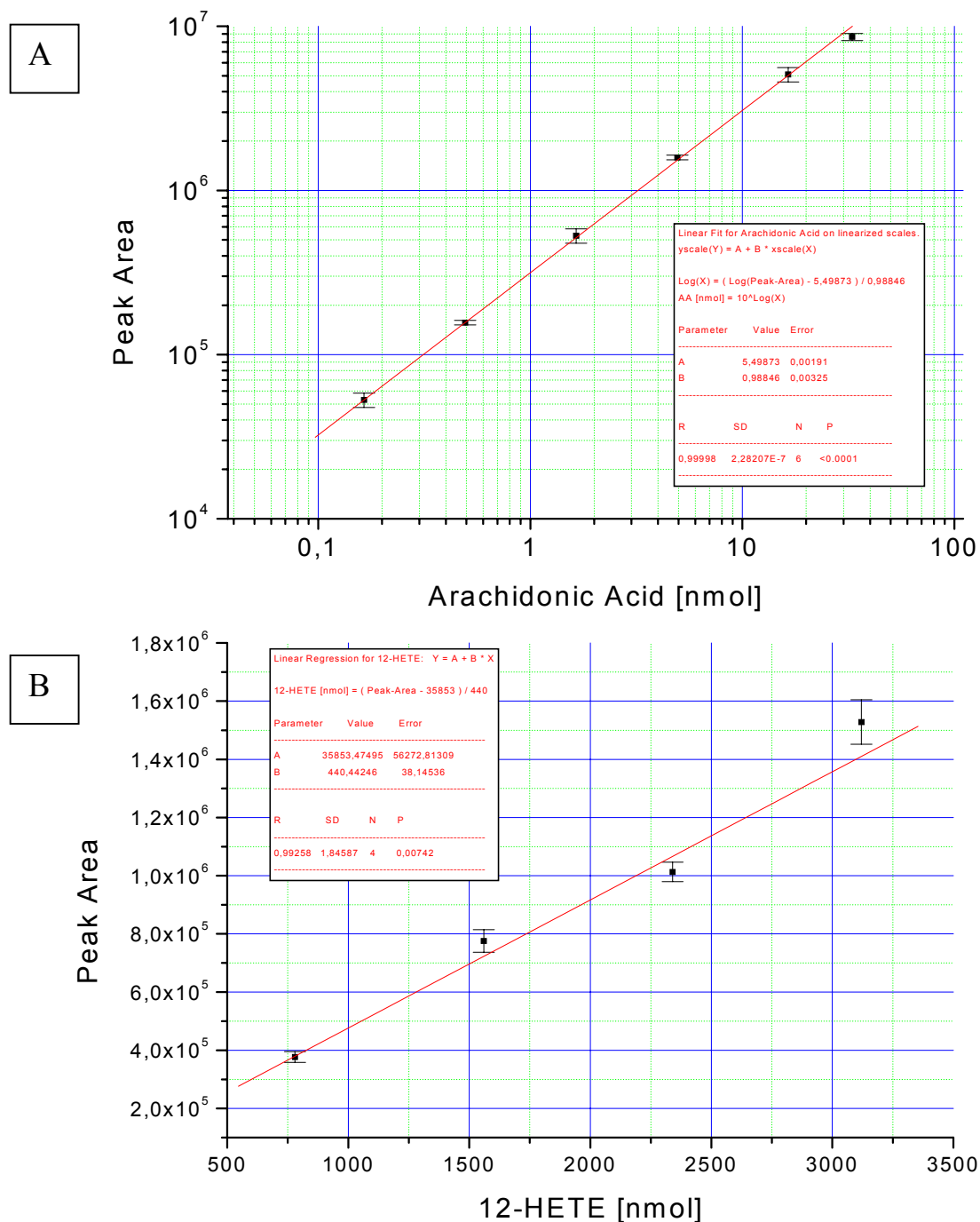


Figure 7. HPLC derived calibration curves for the quantification of AA (A) and 12-HETE (B). (Straight phase Supelcosil LC-S1 column (250 x 46 mm; 5  $\mu\text{m}$  particle size), solvent system : n-hexane:i-propanol:acetic acid (100:2:1, v/v/v), flow rate 1 ml/min).

### 3.2.3 Identification of the end products by GC-MS and quantification

The extraction and sample preparation technique used for HPLC analysis of the arachidonic acid cascade metabolites does not allow the examination of the formation of the hepoxilins. Hepoxilin A<sub>3</sub> and B<sub>3</sub> exhibit very weak UV absorption. GC-MS analysis does not allow the formation of 12-HpETE to be examined due to chemical instability of the hydroperoxy group. Both techniques were used as auxiliary techniques to examine the formation of products from the 12-LOX pathway.

An authentic standard of acid hydrolysed HXA<sub>3</sub> and authentic HXB<sub>3</sub> were derivatised to their corresponding silylated, methyl esters as described under Materials and Methods and analysed by GC-MS. Figure 8a and b represent the mass spectra and fragmentation patterns of 8, 9, 12-TriHETrE (Trioxilin A<sub>3</sub>) and HXB<sub>3</sub> respectively.

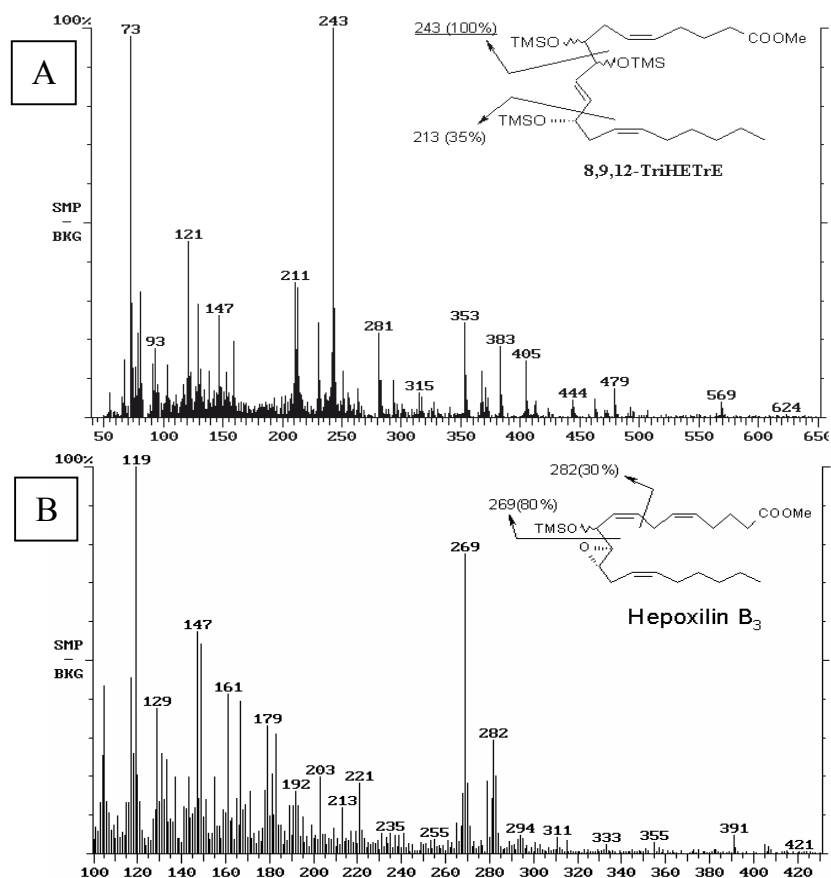


Figure 8. Mass spectra and fragmentation patterns of 8, 9, 12-TriHETrE (A) and hepoxilin B<sub>3</sub> (B) derived from authentic standards. Samples were derivatised as described in Materials and Methods and analysed using a Varian Saturn 4D GC-MS-MS (Supelco DB5-MS column).

The authentic standards were used to plot calibration curves for trioxilin A<sub>3</sub> and HXB<sub>3</sub> (figure 9a and b respectively).

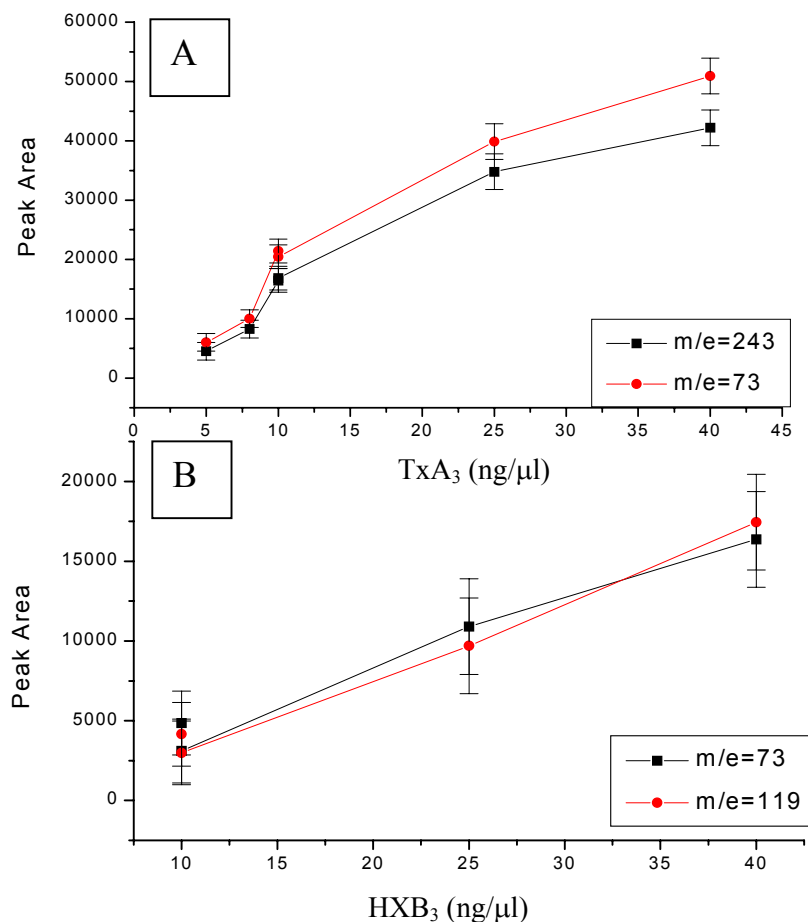


Figure 9. GC-MS derived calibration curves of trioxilin A<sub>3</sub> (A) and hepoxilin B<sub>3</sub> (B). For further details see figure 8.

The deviation from the expected linear shape of the graph can be explained by the low number of estimations ( $n = 3$ ). These were sufficient to allow quantification of the amounts of hepoxilins produced in the biological systems studied.

### **3.3 REGULATORY ROLE OF SELENOENZYMES ON THE 12-LOX PATHWAY**

#### **3.3.1 Both GPx-1 and PHGPx reduce 12-HpETE *in vitro***

To determine whether both GPx-1 and PHGPx of human platelet origin are responsible for the reduction of 12-HpETE to 12-HETE, the cytosol fraction was fractionated on a Sephadex G-100 (super fine) column in 50 mM Tris-HCl buffer (pH 7.5). Two glutathione peroxidase fractions active towards hydrogen peroxide, representing GPx-1 ( $M_r \sim 90$  kDa) and PHGPx ( $M_r \sim 23$  kDa), were obtained (Fig. 10). The shape of the protein concentration/fraction curve

closely resembled that of the total GPx-1 activity/fraction curve.

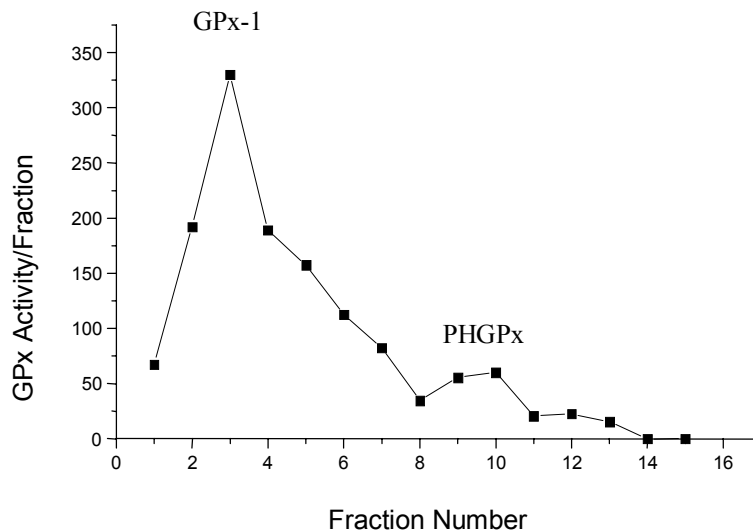


Figure 10. Glutathione peroxidase activity in human platelet cytosol fractions. The cytosol was fractionated on a Sephadex G-100 column and activity measured with  $\text{H}_2\text{O}_2$  as substrate. Activity is expressed as  $[(\Delta \text{ Abs } 340 \text{ nm} \cdot \text{min}^{-1} \times 1000) \times \text{fraction volume}]$ .

Fractions 2-4 and 9/10, representing GPx-1 and PHGPx respectively, were pooled and tested for glutathione-dependent 12-HpETE reductase activity. Both glutathione peroxidases proved to be active (Fig. 11). The enzyme activities of GPx-1 and PHGPx, using 12-HpETE as substrate, were determined to be 11.3 and 0.19 nkat/mg protein respectively. The ratio of GPx-1:PHGPx activity using 12-HpETE as substrate was found to be approximately 60:1. This ratio is similar to that obtained for GPx-1:PHGPx using  $\text{H}_2\text{O}_2$  and PAPC-OOH as substrate (see Table 1). These data reveal that among the selenoenzymes the GPx-1 is the prominent 12-HpETE reductase. Nevertheless PHGPx can be substituted for GPx-1 with respect to this activity, albeit with an enzymatic capacity being more than one order of magnitude lower.

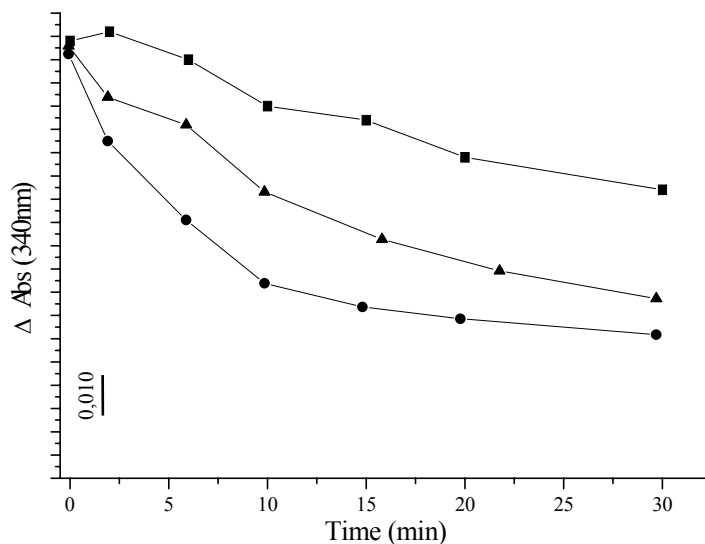


Figure 11. GPx-1 and PHGPx activity in human platelet fractions using 12-HpETE as substrate. The fractions 2-4 (●) and 9/10 (▲), representing GPx-1 and PHGPx respectively (see Fig. 10), were incubated with 20  $\mu$ M 12-HpETE (■, Blank) at 25°C.

### **3.3.2 Role of selenoenzymes in regulating the 12-LOX pathway *in vivo***

To analyse the metabolism of arachidonic acid *in vivo*, human platelets were incubated with 130  $\mu$ M arachidonic acid, the samples extracted as previously described and analysed by HPLC. Human platelets treated with AA produced large amounts of 12-HETE (Fig. 12a). 12-HpETE was detected in one of six independent experiments. To determine the role of selenium-dependent glutathione peroxidases in the regulation of the 12-LOX pathway, the cells were pre-treated for 10 min with 2 mM iodoacetate. [In A431 cells, 2 mM iodoacetate has previously been shown to strongly inhibit PHGPx activity without affecting 12-LOX activity.] In the iodoacetate-treated platelets (Fig. 12b), both 12-HETE and 12-HpETE were detected. This observation provides strong evidence for the role of glutathione peroxidases in regulating the 12-LOX pathway in human platelets. Pre-treatment of the platelets with the 12-LOX inhibitor, ETYA, inhibited the formation of 12-HETE by 100%. This indicates that the platelets contain a functionally active 12-LOX and the activity is not destroyed during isolation of the platelets.

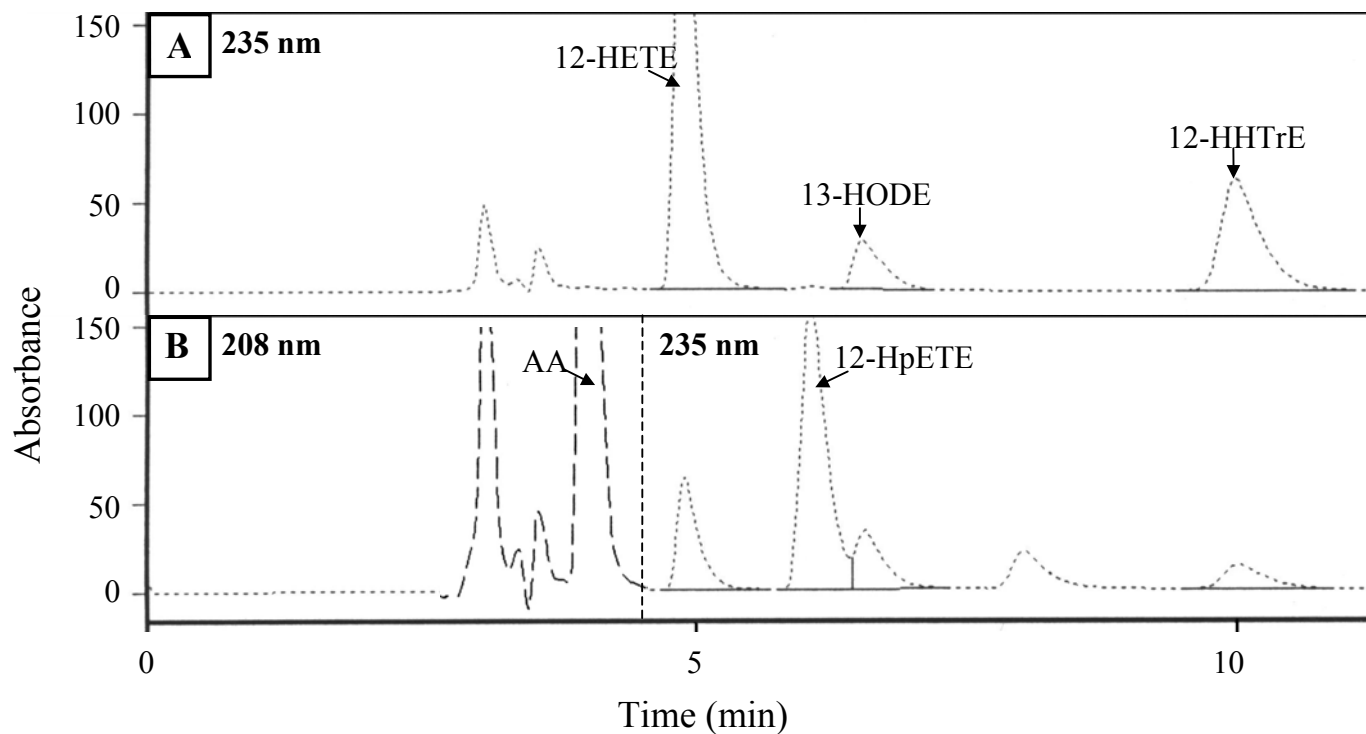


Figure 12. Typical HPLC profiles from platelet extracts incubated with 130  $\mu$ M AA (A) and 2 mM iodoacetate + 130  $\mu$ M AA (B). (Straight phase Supelcosil LC-S1 column (250 x 46 mm; 5  $\mu$ m particle size), solvent system : n-hexane:i-propanol:acetic acid (100:2:1, v/v/v), flow rate 1 ml/min).

The products were quantified by peak area using the calibration curves plotted with authentic standards and normalised for the internal standard 13-HODE (Table 3). The quantities of 12-HETE and 12-HHTrE were both inhibited by 81% in the presence of iodoacetate. A 100 fold increase in the quantity of 12-HpETE was observed in the presence of iodoacetate.

Table 3. Effect of iodoacetate on arachidonic acid metabolism in human platelets (Means  $\pm$  SEM are given, number of experiments are indicated in parentheses). For further details see figure 12.

Metabolite (nmoles)	130 $\mu$ M AA	2 mM iodoacetate + 130 $\mu$ M AA
Arachidonic acid	32.1 $\pm$ 2.7 (4)	35.9 $\pm$ 2.5 (4)
12-HETE	18.6 $\pm$ 1.9 (6)	3.5 $\pm$ 0.5 (6)
12-HpETE	0.1 $\pm$ 0.1 (6)	10.5 $\pm$ 1.6 (5)
12-HHTrE	4.7 $\pm$ 1.3 (6)	0.9 $\pm$ 0.2 (4)

### **3.3.3 Distinct roles for GPx-1 and PHGPx on 12-HpETE reduction**

In rat basophilic cells (Weitzel and Wendel, 1993) GPx-1 has been shown to be more sensitive to selenium deficiency than PHGPx and the PHGPx activity is more rapidly restored upon replenishment by selenium. To evaluate the distinct roles of GPx-1 and PHGPx in the 12-LOX pathway, selenium deficient and partially replenished UT-7 cells were prepared. UT-7 cells were cultured in IMEM/0.75% FCS/10 ng/ml GM-CSF for 20 days (doubling time 66 h) to generate a selenium deficiency. Under these conditions, cells were obtained which exhibited no measurable GPx-1 activity with *t*-butyl hydroperoxide as substrate but possessed ~80% PHGPx activity still. When the cells were replenished with 250 ng/ml sodium selenite for 2 h the PHGPx activity was restored to ~130% of the normal cells whereas still hardly any GPx-1 activity was detected. The cells were treated with 5  $\mu$ M 12-HpETE and the formation of 12-HETE analysed by straight phase HPLC. After 10 min incubation 100% of the 12-HpETE had been reduced to 12-HETE in the wild type cells as compared to ~50% for the selenium-deficient cells (Fig. 13a and b respectively). Thirty minutes incubation resulted in 90% reduction of the 12-HpETE (Fig. 13c). This observation implies that GPx-1 is primarily responsible for the reduction of 12-HpETE, however, PHGPx is capable of fulfilling this role in the absence of GPx-1, albeit at a slower rate as compared to wild-type cells.

It has been reported (Tiedge *et al.*, 1997) that the rat pancreatic cell line RINm5F lacks both GPx-1 and PHGPx activity as determined by Northern blotting. However, PHGPx activity was detected using PAPC-OOH as substrate (Table 1), but no GPx-1 activity was detected. Thus RINm5F cells provided an ideal model for studying the role of PHGPx in the regulation of 12-LOX pathway, since no selenium deficiency is required which may affect other selenoenzymes. RINm5F cells were incubated with 50  $\mu$ M AA for 10 and 30 min in the presence and absence of 2 mM iodoacetate, extracted and analysed by GC-MS. No 12-HETE, Trioxilin A<sub>3</sub> or HXB<sub>3</sub> were detected. As the RINm5F cells possessed no detectable 12-LOX activity, no further experiments were performed.

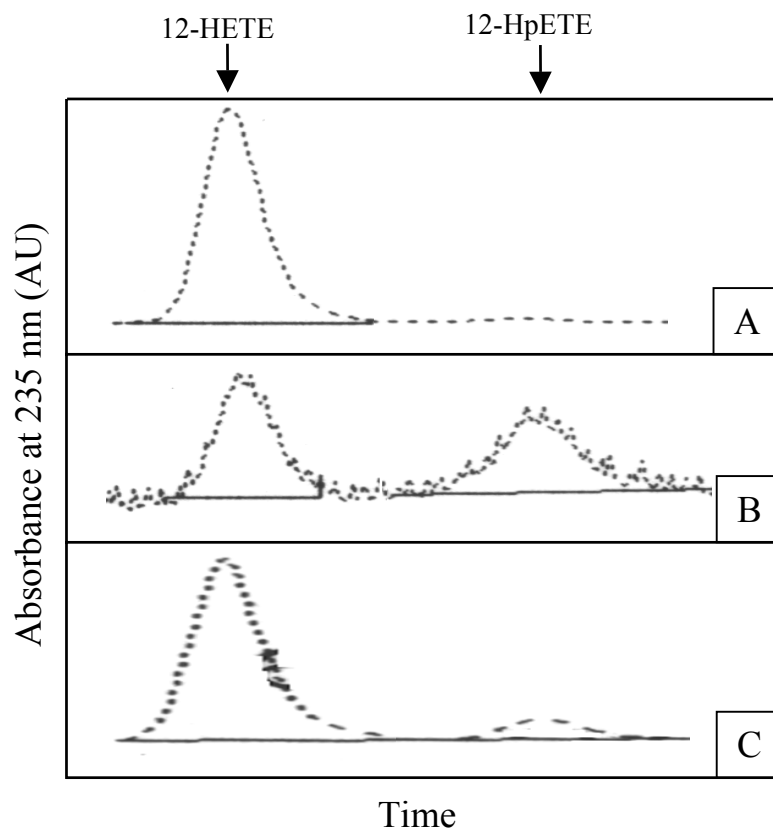


Figure 13. 12-HpETE reduction by wild type UT-7 cells (Tracing A, 5  $\mu$ M 12-HpETE, 10 min at 37°C) and selenium deficient cells (Tracing B and C, 5  $\mu$ M 12-HpETE for 10 min and 30 min respectively at 37°C). Samples were extracted and analysed by HPLC (Straight phase Supelcosil LC-S1 column (250 x 46 mm; 5  $\mu$ m particle size), solvent system : n-hexane:i-propanol:acetic acid (100:2:1, v/v/v), flow rate 1 ml/min).

### **3.4 HEPOXILIN FORMATION IN HUMAN PLATELETS**

#### **3.4.1 Hepoxilin formation with Arachidonic Acid as Substrate**

To analyse the formation of hepoxilin A<sub>3</sub> and B<sub>3</sub> via the 12-lipoxygenase pathway, human platelets were incubated with 100  $\mu$ M arachidonic acid for 10 and 30 min. After 10 min and 30 min incubation with AA, no trioxilin A<sub>3</sub> and HXB<sub>3</sub> were detected.

A large amount of 12-HETE was detected in the samples treated with 100  $\mu$ M AA for 30 min (Fig. 14a). In the platelets pre-treated with 10 $\mu$ M ETYA, the formation of 12-HETE was inhibited by 100% (Fig. 14b).

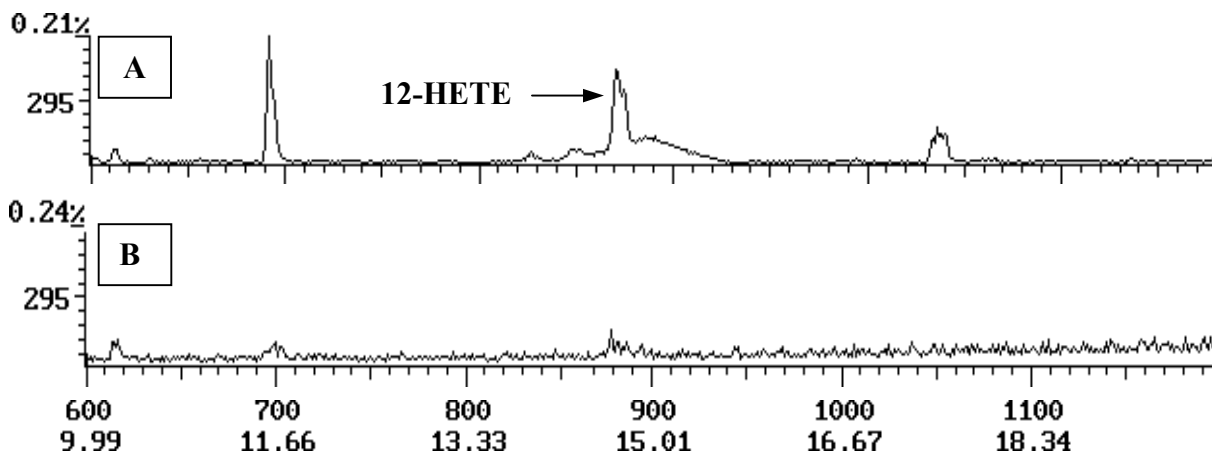


Figure 14. GC-MS profile of the characteristic ion 295 of 12-HETE in human platelet extracts treated with AA in the absence (A) and presence (B) of the 12-LOX inhibitor ETYA. Washed platelets ( $1 \times 10^9$  cells/ml) were treated with 100  $\mu$ M AA for 30 min, extracted and analysed by GC-MS (Varian Saturn 4D GC-MS-MS, Supelco DB5-MS column).

To examine the effect of the selenium-containing glutathione peroxidases in the formation of the hepxilins, human platelets were treated with 100  $\mu$ M AA in the absence and presence of iodoacetate. No trioxilin A<sub>3</sub> was detected, within the limits of the detection method, in the samples treated with AA alone (Fig.15a). By contrast, in the samples pre-treated with 2 mM iodoacetate, sizeable amounts of trioxilin A<sub>3</sub> were detected (Fig. 15b).

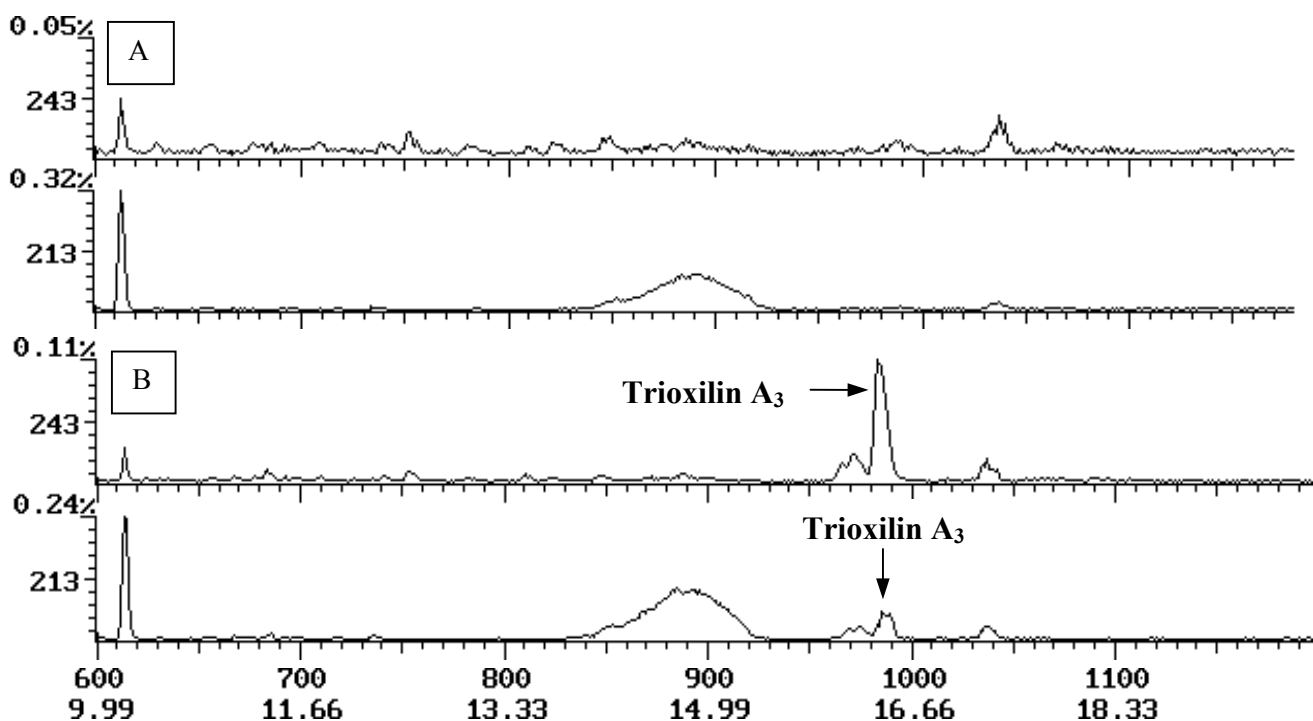


Figure 15. GC-MS profile of the characteristic ions 243 and 213 of trioxilin A<sub>3</sub> in human platelet extracts treated with 100  $\mu$ M AA in the absence (A) and presence of 2 mM iodoacetate (B). (Varian Saturn 4D GC-MS-MS, Supelco DB5-MS column).

Similarly, no HXB<sub>3</sub> was detected in the samples treated with AA alone (Fig. 16a). But, hepoxilin B<sub>3</sub> was detected in the samples pre-treated with iodoacetate (Fig. 16b).

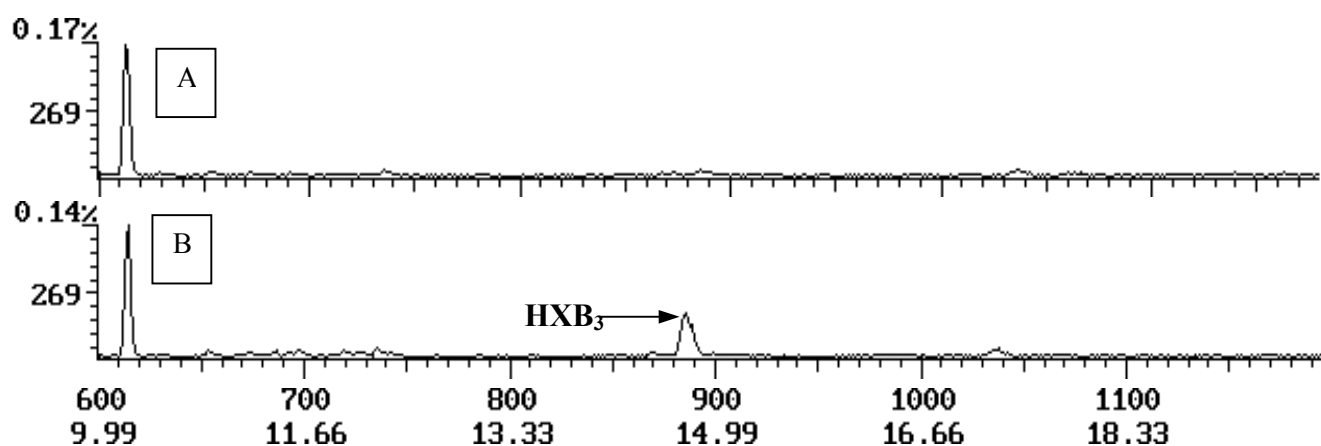


Figure 16. GC-MS profile of the characteristic ion 269 of HXB<sub>3</sub> in human platelet extracts treated with 100  $\mu$ M AA in the absence (A) and presence of 2 mM iodoacetate (B). (Varian Saturn 4D GC-MS-MS, Supelco DB5-MS column).

The formation of the hepoxilins in human platelets incubated with 100  $\mu\text{M}$  AA and the various inhibitors is summarised in Table 4. The ratio of trioxilin A<sub>3</sub> to HXB<sub>3</sub> in the presence of iodoacetate was found to be 1:3.75 thus excluding a specific HXA<sub>3</sub> synthase in human platelets. Sodium cyanide (2 mM), an inhibitor of the pseudolipohydroperoxidase activity of haemoglobin, did not inhibit hepoxilin formation thus not supporting the involvement of haemin catalysis in this process in human platelets.

Table 4. Hepoxilin formation in human platelets treated with 100  $\mu\text{M}$  AA. For further details see figure 15. (The amounts were quantified by peak area using calibration curves with authentic standards, n = 4).

Inhibitor(s)	8,9,12/8,11,12-TriHETrE (nmol)	HXB <sub>3</sub> (nmol)
none	0	0
10 $\mu\text{M}$ ETYA	0	0
2mM iodoacetate	0.4 $\pm$ 0.1	1.5 $\pm$ 0.1
2mM iodoacetate 2mM cyanide	1.0 $\pm$ 0.1	2.0 $\pm$ 0.1

#### 3.4.1.1 IDENTIFICATION OF TWO ISOMERS OF TRIOXILIN A<sub>3</sub> :- 8,11,12-TriHETrE AND 8,9,12-TriHETrE

Hepoxilin B<sub>3</sub> is relatively stable to hydrolysis and the mass spectrum from the samples corresponded well to the authentic standard (Fig 8b). The hydrolysis of HXA<sub>3</sub> occurs more readily due to the epoxide ring in an allyl position and gives rise to a more complex product pattern. Under the experimental conditions used, the mass spectrum of trioxilin A<sub>3</sub> was found to be variable with respect to the fragmentation pattern. Different cell preparations resulted in a maximum at either 213, 243 or variable amounts of both (Fig. 17, compare to Fig. 8a). From these results we therefore propose that two isomers of trioxilin A<sub>3</sub> occur, namely 8,11,12-TriHETrE and 8,9,12-TriHETrE, as derived from the fragmentation pattern (Fig. 17, insert). All further use of the name trioxilin A<sub>3</sub> refers to both isomers.

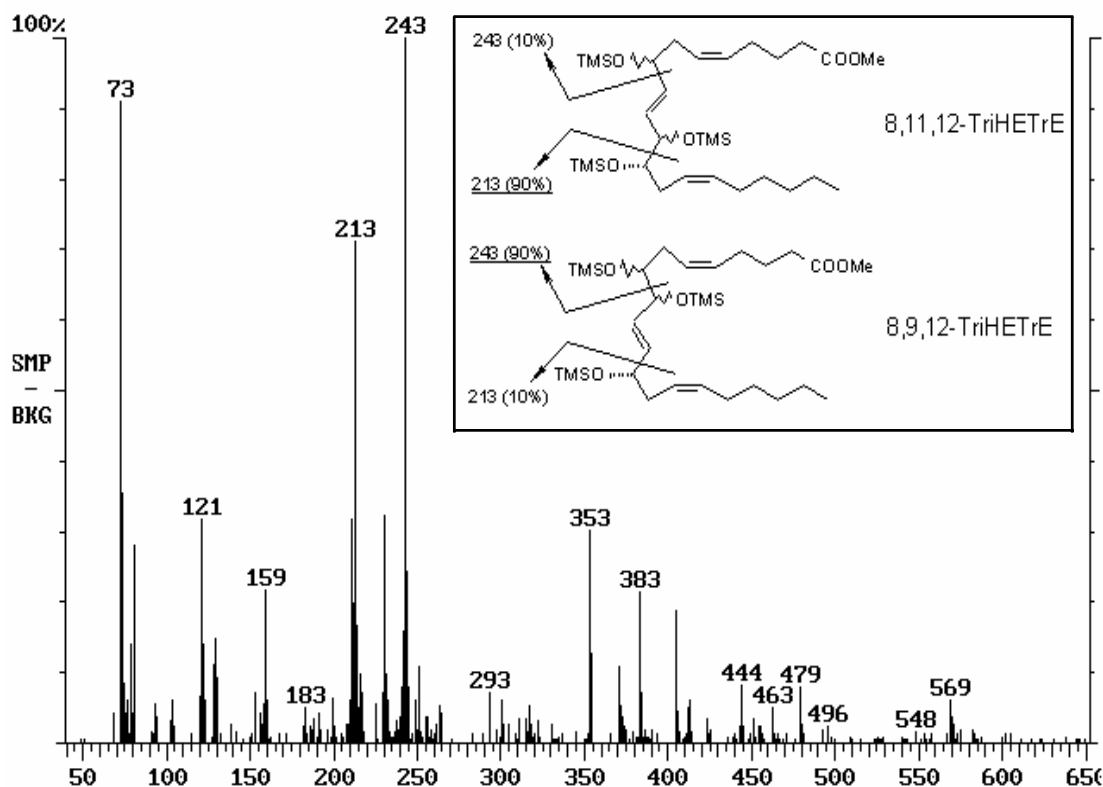


Figure 17. Mass spectrum and fragmentation pattern of the two proposed isomers of Trioxilin A<sub>3</sub>, namely 8,11,12-TriHETrE and 8,9,12-TriHETrE. (Varian Saturn 4D GC-MS-MS (Supelco DB5-MS column).

From these results it was decided to use the mass fragments 213/243 for the quantification of the two isomers of trioxilin A<sub>3</sub> and 119/269 for the quantification of HXB<sub>3</sub>.

### 3.4.2 Hepoxilin formation from 12-HpETE

In all samples treated with 20 or 50  $\mu$ M 12-HpETE, in the absence of iodoacetate, the formation of the hepoxilins and 12-HETE was observed (GC-MS profiles not shown, Table 5). The product pattern was similar to that shown in Fig. 15b and 16b using human platelets incubated with AA. From these results, in conjunction with the HPLC results, one could speculate that the hepoxilins are only formed in human platelets above a certain threshold concentration of 12-HpETE. The formation of 8,9,12/8,11,12-TriHETrE in platelets treated with 50  $\mu$ M 12-HpETE was approximately 4 $\times$  higher than that from 20  $\mu$ M thus adding support to a threshold concentration.

Table 5. Trioxilin A<sub>3</sub>, HXB<sub>3</sub> and 12-HETE formation in human platelets incubated with 12-HpETE as substrate. (The amounts were quantified by peak area using calibration curves with authentic standards, n = 4).

12-HpETE	Inhibitor(s)	8,9,12/8,11,12-TriHETrE (nmol)	HXB <sub>3</sub> (nmol)	12-HETE (area units)
20 μM	None	0.4 ± 0.1	present <sup>a</sup>	87.7 ± 2
20 μM	10 μM ETYA	0.3 ± 0.1	present <sup>a</sup>	48.1 ± 2
20 μM	2 mM cyanide	0.4 ± 0.1	present <sup>a</sup>	86.4 ± 1
20 μM	10 μM ETYA 2 mM cyanide	0.3 ± 0.1	present <sup>a</sup>	40.8 ± 1
50 μM	None	1.6 ± 0.3	3.0 ± 0.3	100.7 ± 3
50 μM	10 μM ETYA	0.9 ± 0.3	1.2 ± 0.3	15.1 ± 1.5

a: co-migrating peak, quantification not possible.

In the presence of iodoacetate, the reduction of 12-HpETE to 12-HETE was inhibited by 65% (Table 6). The inhibitory effect with 12-HpETE as substrate is lower than when AA is used as substrate. This supports the hypothesis that GPx-1 and PHGPx play an important role in regulating the 12-LOX pathway. The 12-LOX inhibitor, ETYA, had no effect on the reduction of 12-HpETE, thus ruling out the role of 12-LOX in 12-HpETE reduction (see section:- Hepoxilin formation by platelet- and leukocyte type 12-LOX).

Table 6. Effect of 2 mM iodoacetate and 10 μM ETYA on 20 μM 12-HpETE reduction in platelets ( $3.2 \times 10^8$  cells/ml). (Straight phase Supelcosil LC-S1 column (250 x 46 mm; 5 μm particle size), solvent system : n-hexane:i-propanol:acetic acid (100:2:1, v/v/v), flow rate 1 ml/min). (Results expressed as mean % peak area, n = 2).

INHIBITOR		12-HETE	12-HpETE
Iodoacetate	ETYA		
-	-	100	0
+	-	35	65
-	+	100	0
+	+	38	62

### **3.5 HEPOXILIN FORMATION IN OTHER CELL SYSTEMS**

#### **3.5.1 The Megakaryoblast Cell Line UT-7**

From the data in Table 1 it is evident that platelets and the myeloid leukemia cell line UT-7 exhibit similar GPx-1 and PHGPx activities. Wild type UT-7 cells were treated with 100  $\mu$ M AA for 10 and 30 min, extracted and analysed by HPLC. Neither 12-HETE nor 12-HpETE was detected thus suggesting that UT-7 cells possess no 12-LOX. RT-PCR also failed to detect 12-LOX (Fig. 18).

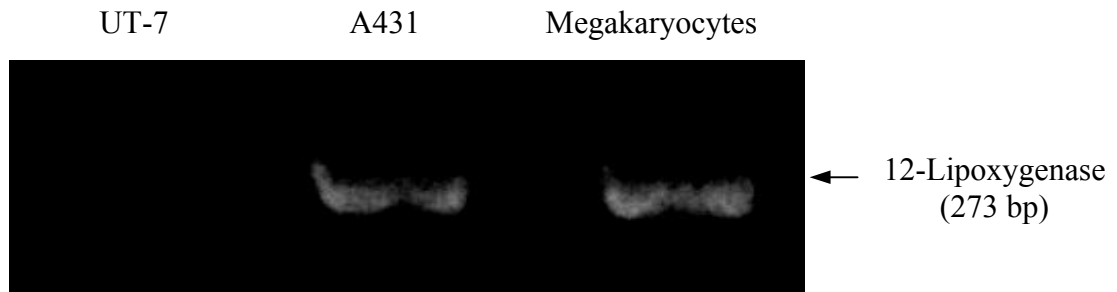


Figure 18. RT-PCR detection of the messenger for 12-LOX in UT-7 cells, A431 cells and megakaryocytes. Isolation of total RNA and RT-PCR were performed as described in Materials and Methods, PCR products were separated on a 2% agarose gel.

Similar results were obtained with UT-7 cells, as compared to human platelets, when incubated with 20 $\mu$ M 12-HpETE. In the absence of 2 mM iodoacetate, UT-7 cells ( $4 \times 10^6$  cells/ml) produced 0.47 nmol trioxilin A<sub>3</sub>. In the presence of iodoacetate, the reduction of 12-HpETE to 12-HETE was inhibited. The inhibitory effect was found to be dependent on the concentration of 12-HpETE added (5 – 20  $\mu$ M, Fig. 19). The lower the 12-HpETE concentration the lower the inhibitory effect, thus suggesting the possibility of a threshold concentration. Above the threshold concentration, the reducing capacity of the cells is exceeded and more 12-HpETE is detected.

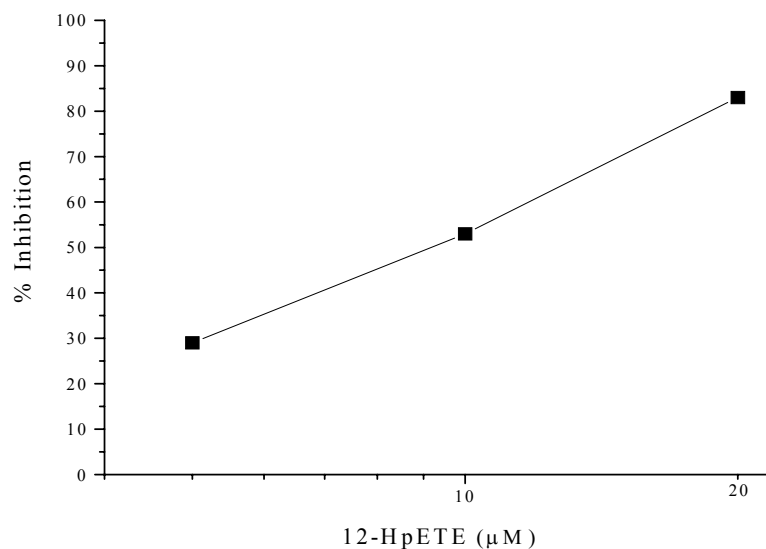


Figure 19. Effect of 12-HpETE concentration on the inhibitory effect by iodoacetate. UT-7 cells ( $3.5 \times 10^6$  cells/ml) were pre-treated with 2 mM iodoacetate (10 min) before the addition of 5, 10 and 20  $\mu$ M 12-HpETE. Results expressed as % peak area 12-HpETE.

As the 12-LOX pathway is bifurcated at the level of 12-HpETE, it may be hypothesised that the increased substrate availability would result in increased hepoxilin synthesis. To investigate this, the formation of hepoxilin in UT-7 cells was examined. In the presence of 2 mM iodoacetate and 20  $\mu$ M 12-HpETE, approximately 10  $\times$  higher concentrations of trioxilin A<sub>3</sub> and HXB<sub>3</sub> were detected (Fig. 20). The peak areas of trioxilin A<sub>3</sub> and HXB<sub>3</sub> in the iodoacetate treated cells lie outside the calibration curve and could thus not be quantified. The above observations support the hypothesis that the level of GPx-1 plus PHGPx and 12-HpETE in the cell determines the amount of 12-HETE and hepoxilins produced.

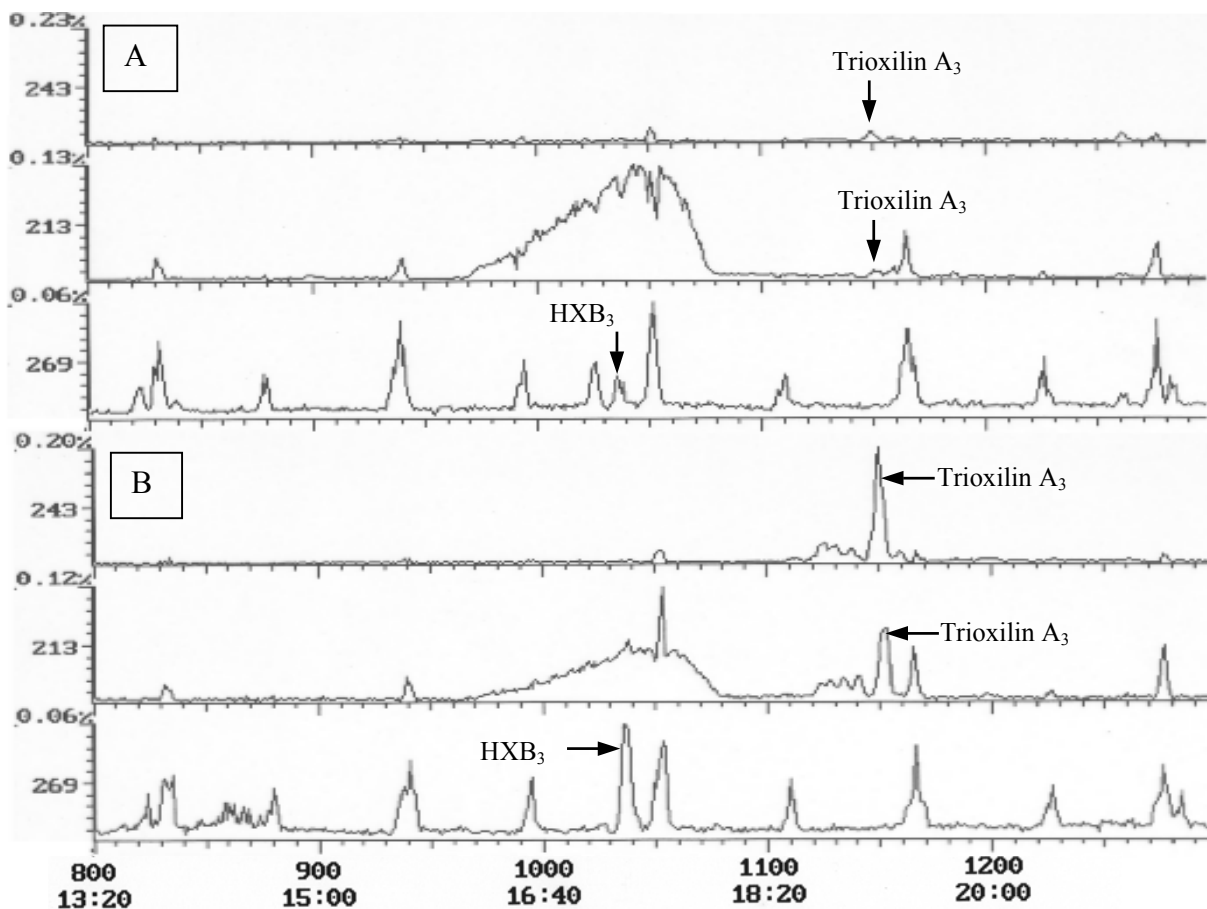


Figure 20. Trioxilin A<sub>3</sub> and HXB<sub>3</sub> formation by wild type UT-7 cells (A) and iodoacetate treated cells (B) incubated with 12-HpETE. GC-MS profiles of the characteristic ions of trioxilin A<sub>3</sub> (243/213) and HXB<sub>3</sub> (269) are presented. UT-7 cells ( $4 \times 10^6$ /ml) were treated with 20  $\mu$ M 12-HpETE in the presence and absence of 2 mM iodoacetate. (Varian Saturn 4D GC-MS-MS, Supelco DB5-MS column).

### 3.5.2 The Epidermoid Tumour Cell Line A431

The role of PHGPx in the regulation of the 12-LOX pathway was also studied in the human epidermoid carcinoma cell line A431. The cells were grown in DMEM/10% FCS until 100% confluence, trypsinated, washed and resuspended at a concentration of  $8-10 \times 10^6$  cells/ml in PBS/BSA/glucose.

#### 3.5.2.1 HEPOXILIN FORMATION FROM ARACHIDONIC ACID

It has been reported in the literature (Huang *et al.*, 1998, 1999a) that in A431 cells PHGPx masks the activity of 12-LOX, therefore the lack of detection of 12-HETE when treated with AA. In agreement with the literature, no 12-HETE was detected when AA (100  $\mu$ M) was used as substrate. This effect is not seen in human platelets that also contain both enzymes in

comparable concentrations. The only difference between A431 cells and platelets with regards to PHGPx is the intracellular distribution of the activity. To investigate the role of PHGPx in masking the 12-LOX activity, the cells were pre-treated with 2 mM iodoacetate for 10 min before the addition of 100  $\mu$ M AA. After 10 and 30 min, the samples were extracted and analysed by GC-MS. No 12-HETE was detected in the samples. The lipoxygenases are activated by an increased peroxide tone. To investigate the role of the hydroperoxide tone in the masking of the 12-LOX activity 3  $\mu$ M *t*-butylhydroperoxide was added 5 s prior to the addition of AA. No 12-HETE, trioxilin A<sub>3</sub> or HXB<sub>3</sub> were detected. The presence of 12-LOX mRNA in A431 was detected by RT-PCR (Fig. 18). This work does not support the assumption of Chen *et al.* (1997) that PHGPx controls 12-LOX activity in A431 cells. Iodoacetate, which has previously been shown to inhibit PHGPx, does not abolish inhibition of 12-LOX product formation. The GPx-1 activity with 12-HpETE as substrate is 60 $\times$  higher than PHGPx. In A431 cells, 12-LOX activity appears to be regulated by a non-selenium enzyme, presumably a particulate enzyme (Chen *et al.*, 1997; Huang *et al.*, 1998).

#### 3.5.2.2 HEPOXILIN FORMATION FROM 12-HpETE

Both untreated A431 cells (Fig. 21a) and heat inactivated cells (65 $^{\circ}$ C for 10 min, Fig. 21b) produced trioxilin A<sub>3</sub> and HXB<sub>3</sub> when 12-HpETE was used as substrate. Due to a co-migrating peak, the peak areas for HXB<sub>3</sub> could not be determined. The heat-inactivated cells produced approximately 2 $\times$  more trioxilin A<sub>3</sub> than the untreated cells. These results suggest that trioxilin A<sub>3</sub> and hepxilin B<sub>3</sub> formation in A431 cells occurs via a non-enzymatic process.

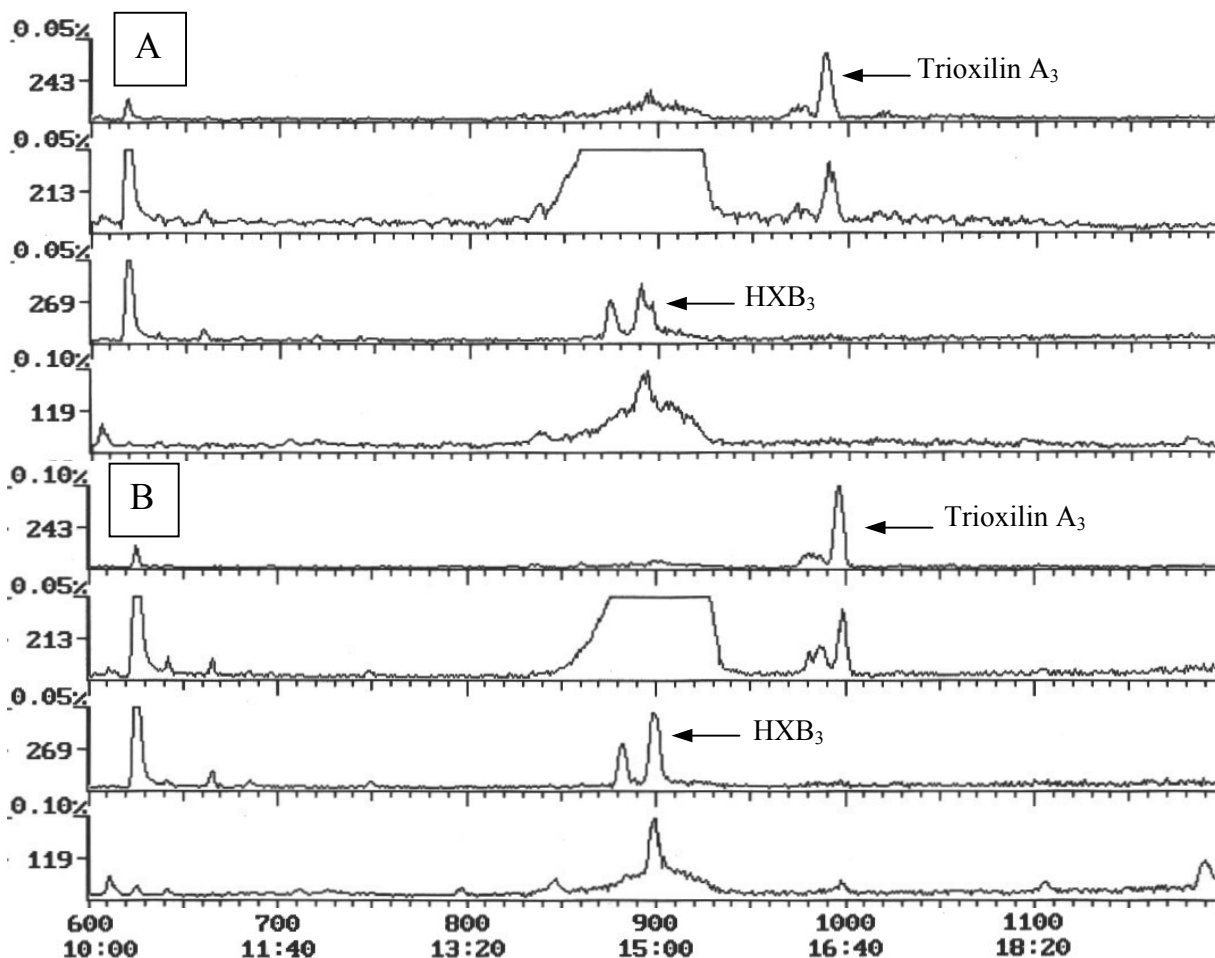


Figure 21. Hepoxilin formation by wild type A431 cells (A) and heat inactivated cells (B). GC-MS profiles of the characteristic ions of trioxilin A<sub>3</sub> (243/213) and HXB<sub>3</sub> (269/119) are presented. Harvested and washed cells were incubated with 50  $\mu$ M 12-HpETE for 10 min, extracted and analysed by GC-MS (Varian Saturn 4D GC-MS-MS, Supelco DB5-MS column).

### **3.6 HEPOXILIN FORMATION BY PLATELET- AND LEUKOCYTE-TYPE 12-LOX**

Since earlier work has clearly shown that both soybean LOX-1 and reticulocyte 15-LOX are capable of converting hydroperoxy-polyenoic fatty acids to their hydroepoxy derivatives, the role of the mammalian LOXs in hepoxilin A<sub>3</sub> and B<sub>3</sub> synthesis was studied.

#### **3.6.1 Oxygen Uptake by Mammalian Lipoxygenases**

Pure human recombinant 12-LOX (platelet type) and porcine leukocyte 12-LOX were incubated with 100  $\mu$ M AA or 50  $\mu$ M 12-HpETE at 37°C and the reactions monitored with a Clarke electrode. Upon starting the reaction by the addition of enzyme, with AA as substrate, an oxygen uptake was measured (Trace not shown, Table 7). The reaction with platelet-type enzyme ceased after 20-30 min whereas the leukocyte-type enzyme was self-inactivated

within 5 min.

Table 7. Oxygen uptake by mammalian lipoxygenases. Enzyme was added to the substrate in an oxygraphic measuring chamber and the oxygen uptake measured using a Clarke electrode as described in Materials and Methods.

	Arachidonic Acid (50 nmol)	12-HpETE (25 nmol)
Platelet 12-lipoxygenase : initial rate (nmol/min)	0.47	0
: total (nmol)	8.6 ± 0.7	0
Leukocyte 12-Lipoxygenase : initial rate (nmol/min)	47.5	0
: total (nmol)	28.5	0

### **3.6.2 Hepoxilin Formation by the Mammalian Lipoxygenases**

All experiments with platelet-type and leukocyte-type enzymes were incubated for 30 and 4.5 min respectively, as determined by oxygraphic measurement. The samples were extracted as described under Materials and Methods and the products identified and quantified by GC-MS (Table 8).

The leukocyte-type 12-LOX formed ~ 2× more trioxilin A<sub>3</sub> and HXB<sub>3</sub> from both AA and 12-HpETE as compared to the platelet-type enzyme. The platelet-type 12-LOX formed ~15× more trioxilin A<sub>3</sub> and HXB<sub>3</sub> with 12-HpETE as substrate than from AA. The sum of trioxilin A<sub>3</sub> and HXB<sub>3</sub> formed from AA was approximately 10% of the 12-HpETE primarily formed. These results clearly show that under certain conditions the mammalian 12-LOX's are capable of forming hepoxilins from AA and 12-HpETE.

Table 8. Hepoxilin formation by mammalian 12-LOX's. Enzyme was added to the substrate in an oxygraphic measuring chamber, after 30 min (platelet enzyme) and 4.5 min (leukocyte enzyme) the reactions were stopped and analysed by GC-MS.

	HXB <sub>3</sub> (ng/μl)	Total HXB <sub>3</sub> in ng and nmol (in parenthesis)	Trioxilin A <sub>3</sub> (ng/μl)	Total Trioxilin A <sub>3</sub> in ng and nmol (in parenthesis)	<b>% conv. to hepoxilins</b> (Trioxilin A <sub>3</sub> + HXB <sub>3</sub> )
leukocyte 12-LOX + 100 μM AA	11 ± 2	1100 ± 200  (2.6 ± 0.47)	7 ± 2	700 ± 200  (1.2 ± 0.34)	<b>7.6 ± 1.8</b>
platelet 12-LOX + 100 μM AA	0	0	3 ± 2	300 ± 200  (0.51 ± 0.34)	<b>1.0 ± 0.7</b>
leukocyte 12-LOX + 50 μM 12-HpETE	12 ± 2	1200 ± 200  (2.8 ± 0.47)	15 ± 2	1500 ± 200  (2.6 ± 0.34)	<b>21.6 ± 1.8</b>
platelet 12-LOX + 50 μM 12-HpETE	10 ± 2	1000 ± 200  (2.4 ± 0.47)	8 ± 2	800 ± 200  (1.4 ± 0.34)	<b>15.2 ± 1.8</b>

### **3.6.3 Effect of Inactivation of Mammalian Lipoxygenases on Hepoxilin Formation**

Inactivation of the platelet-type enzyme with ETYA (10 μM for 10 min) or by heat (65°C for 10 min) resulted in a partial inhibition of the conversion of 12-HpETE to trioxilin A<sub>3</sub>, hepoxilin B<sub>3</sub> and 12-HETE (Table 9). No inhibition of product formation was observed when the leukocyte-type enzyme was inactivated. These results suggest that mammalian 12-LOX is competent for the conversion of 12-HpETE to the hepoxilins by virtue of its lipohydroperoxidase activity.

Table 9. Hepoxilin formation by pseudolipohydroperoxidase activity of mammalian 12-LOX's. Enzymes were inactivated by either 10  $\mu$ M ETYA (37°C, 5 min) or heat (65°C for 10 min) and incubated with 20  $\mu$ M 12-HpETE under the same conditions as described in Table 8. Results expressed as percentage of peak area compared to the control.

12-Lipoxygenase	Inactivation	8,9,12/8,11,12-TriHETrE	12-HETE
Human platelet type	None	100	100
	Heat	40	52
	ETYA	75	40
Porcine leukocyte type	None	100	100
	Heat	101	103
	ETYA	112	97

### **3.7 BIOLOGICAL EFFECTS OF HXA<sub>3</sub> ON TUMOUR CELLS**

#### **3.7.1 Effect of Eicosanoids on PHGPx mRNA Transcription**

The above results clearly indicate that the formation of hepoxilin is regulated at the level of the 12-LOX pathway in a multiple manner. One of the controlling enzymes is the PHGPx. Therefore we decided to look at the role of the 12-LOX products in regulating PHGPx at the transcription level. A431 and HeLa cells were grown to ~70% confluence, washed and treated with various eicosanoids (1  $\mu$ M final concentration, Table 10). Quantitative RT-PCR revealed that all the products caused an increase in the amount of PHGPx mRNA except for AA in HeLa cells (Table 10). HeLa cells lack 12- and 15-LOX. The negative effect by AA and positive effect by the hydroxy and hydroperoxy-fatty acids thus support the fact that the LOX end-products are directly responsible for regulating PHGPx mRNA expression. The level of induction by the eicosanoids varied from 40 to 300%. The basal level of mRNA in the controls varied between experiments. This was initially thought to be due to differences in the amount of selenium present in the different batches of FCS. To overcome this the medium was supplemented with 50 nM Na<sub>2</sub>SeO<sub>3</sub>. By this way, the basal level of PHGPx mRNA was found to be more consistent between different experiments. Nevertheless, the extent of induction still varied between various cell batches. This induction was consistently observed. The variation may be possibly due to the time dependence (see below).

Table 10. Effect of various eicosanoids (1  $\mu$ M) on the induction of PHGPx mRNA in the tumour cell lines A431 and HeLa. Cells were grown to ~70% confluence, incubated for 4 h with the various eicosanoids and quantitative RT-PCR performed as described in Materials and Methods.

Eicosanoid	A431*	HeLa
Arachidonic Acid	+	-
HXA <sub>3</sub>	++	++
12-HpETE	++	++
12-HETE	++	++
ETYA	-	-
5-HPETE	nd	++

(- = weak/no induction, + = 50% induction, ++ =  $\geq$  100% induction, nd = not determined)

The above data suggest that eicosanoids of the 12-LOX pathway regulate the expression of PHGPx. This effect is not cell-specific as seen by the increase in PHGPx mRNA levels in HeLa cells that lack 12- and 15-LOX.

### **3.7.1.1 Dose-dependent effect of HXA<sub>3</sub> on PHGPx mRNA transcription**

The induction of PHGPx mRNA by HXA<sub>3</sub> was found to be concentration dependent. Figure 22 shows a representative gel of the concentration dependent effect of HXA<sub>3</sub> on PHGPx mRNA expression in A431 cells. Due to large differences in the level of induction between different cell batches, the threshold concentration and ED50 are estimated to be ~50 nM and 100-300 nM respectively.

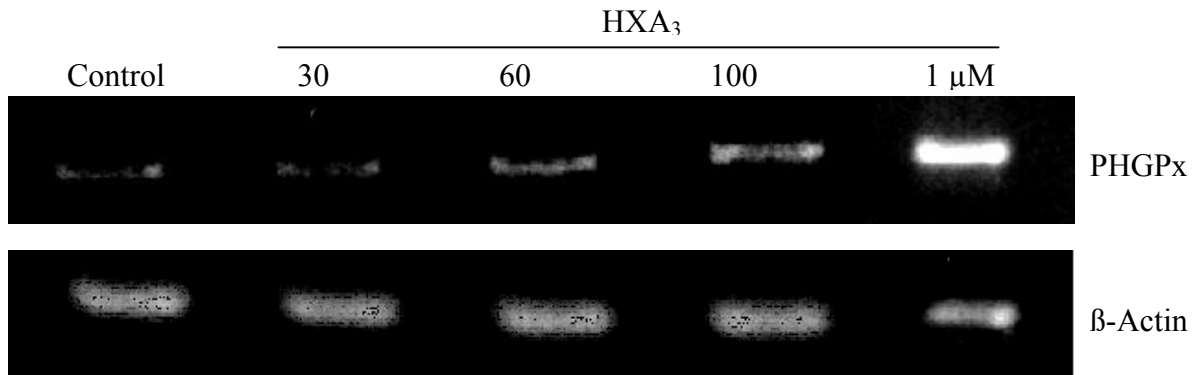


Figure 22. Concentration dependent effect of HXA<sub>3</sub> on PHGPx mRNA levels in A431 cells. Cells were treated with various concentrations of HXA<sub>3</sub> under the same conditions as described in Table 10. β-actin was used as standard for comparison.

### 3.7.1.2 Time Course of PHGPx mRNA Induction

A previous study (Schnurr *et al.*, 1999a) has shown that IL-4 stimulation causes a decrease in PHGPx expression in A549 cells after 24 h. As a clear increase in PHGPx mRNA expression was observed in our hands after 4 h, the time course of PHGPx mRNA transcription was studied. Due to the shorter doubling time of HeLa cells (~48 h) compared to A431 cells (80-100 h), they were preferred for the study. The cells were grown to ~70% confluence, washed and treated with 1 μM 12-HpETE for 4, 8, 16 and 24 h, the total RNA was prepared and subjected to quantitative RT-PCR. Results were normalised using β-actin. Figure 23 shows the time course of PHGPx expression in HeLa cells. The time course revealed a biphasic pattern in that after 4 h an up-regulation was detected. After 24 h, the level of PHGPx mRNA was down-regulated as compared to the untreated cells.

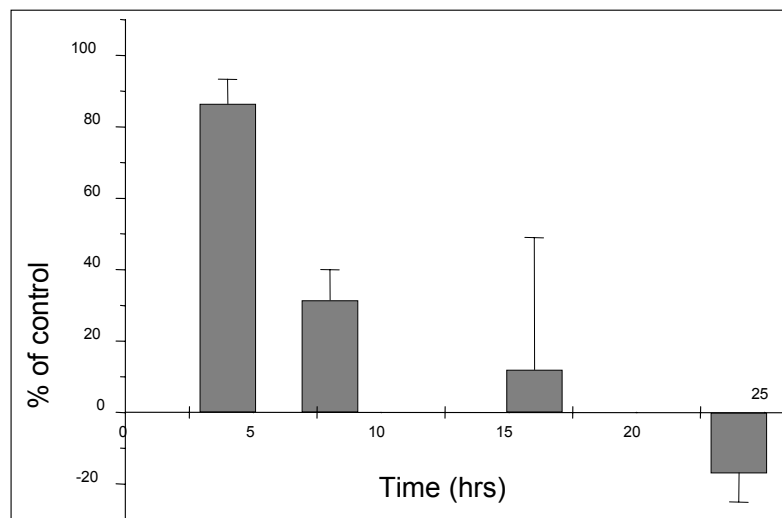


Figure 23. Time course of PHGPx mRNA transcription in HeLa cells treated with 1  $\mu$ M 12-HpETE. HeLa cells were grown to  $\sim$  70% confluence, washed and incubated with 12-HpETE for varying times. The total mRNA was isolated and analysed as described in Table 10. Mean values  $\pm$  SEM for three estimations are given.

### **3.7.2 Effect of HXA<sub>3</sub> on Cell Proliferation**

The 12-LOX product 12-HETE has been reported to play a significant role in cancer metastasis (for review see Honn *et al.*, 1994a; Tang and Honn, 1999). To determine the effect of HXA<sub>3</sub> and other 12-LOX products on cell proliferation, A431 and HeLa cells were cultured in DMEM/10% FCS until  $\sim$ 60-70% confluence and synchronised by further culturing in medium containing 1% FCS. Two different incubation conditions were used. Firstly, at time 0, DMEM/1% FCS was added containing the eicosanoids and incubated for 4 h. The medium was aspirated and DMEM/20% FCS/0.5  $\mu$ Ci <sup>3</sup>H-Thymidine was added. After 24, 48 and 72 h the medium was aspirated, the cells washed 3 $\times$  with PBS, harvested and the incorporated radioactivity measured (Fig. 24). All the 12-LOX products examined, at a concentration of 1  $\mu$ M, resulted in an increase in thymidine incorporation. This effect appears to be concentration dependent as 0.1  $\mu$ M 12-HETE had no significant effect.

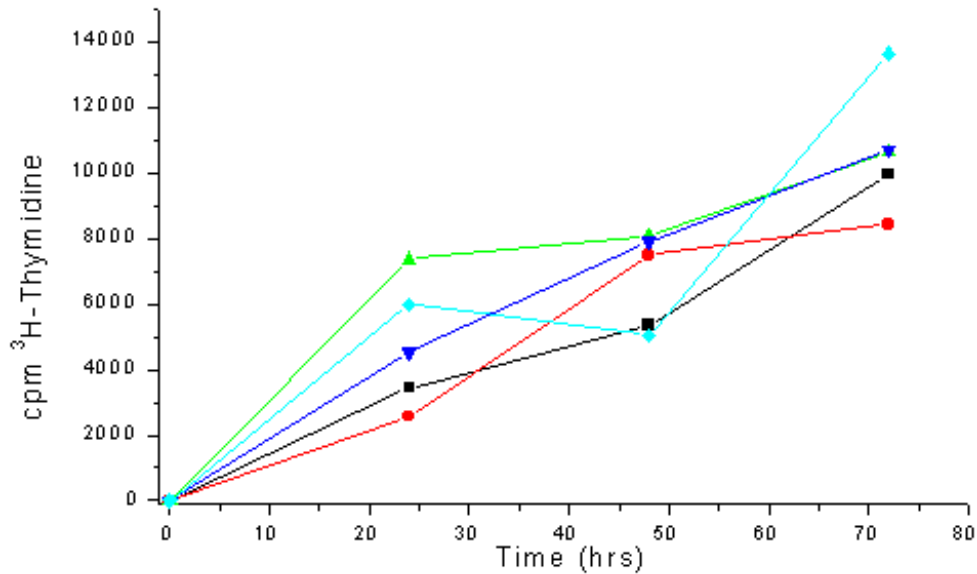


Figure 24. Effect of 12-LOX pathway products on A431 cell proliferation as measured by  $^3\text{H}$ -Thymidine incorporation. (Blank ■, 0.1  $\mu\text{M}$  12-HETE ●, 1  $\mu\text{M}$  12-HETE ▼, 1  $\mu\text{M}$  HXA<sub>3</sub> ▲, 1  $\mu\text{M}$  12-HpETE ◆). Synchronised cells were treated with the eicosanoids in DMEM/1% FCS for 4 h before the addition of DMEM/20% FCS/0.5  $\mu\text{Ci}$   $^3\text{H}$ -Thymidine. (Representative plot of 3 separate experiments showing identical time courses).

In a second set of experiments, the cells were treated with 1  $\mu\text{M}$  12-HETE in DMEM/20% FCS at time 0 (Fig. 25a) or after 24 h incubation in DMEM/20% FCS (Fig. 25b). From the results it can be clearly seen that the cell proliferatory effect of 12-HETE is retarded by up to 24 h when added to cells in DMEM/20% FCS as compared to when added to cells in serum poor medium. This may be due to the high FCS concentration initially masking or binding the 12-HETE. Albumin has been suggested to play an important role in the regulation of the availability of substrates and modify the metabolism of hydroxyeicosatetraenoic acids via 12-LOX in human platelets (Dadaian and Westlund, 1999).

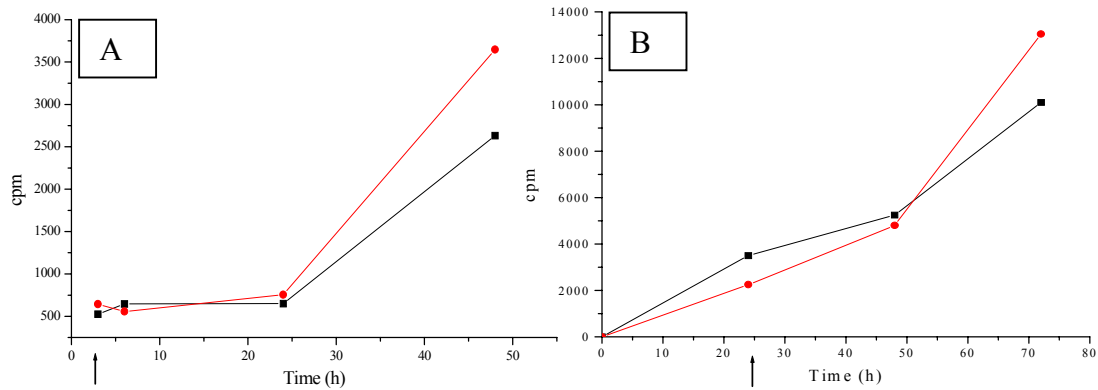


Figure 25. Effect of FCS on 12-HETE induced A431 cell proliferation. Synchronised cells (■) were treated with 1  $\mu$ M 12-HETE (●) either at time 0 in DMEM/20% FCS (A,  $n = 2$ ) or after 24 h incubation in DMEM/20% FCS (B, representative of 3 experiments) ( $\uparrow$  indicates time of addition of 12-HETE).

To determine whether these effects were solely due to the exogenously added products or induction of the 12-LOX pathway and endogenously produced 12-LOX products, the cells were treated with 1  $\mu$ M 12-HpETE, 12-HETE or HXA<sub>3</sub> and the known 12-LOX inhibitor ETYA. No conclusive results were obtained as ETYA alone caused an increase in <sup>3</sup>H-thymidine incorporation. The inhibitor ETYA is known to activate peroxisome-proliferator-activator receptors (PPAR's).

## **II BIOLOGICAL ACTIONS OF HXA<sub>3</sub> ON HUMAN NEUTROPHILS**

### **3.8 Chemotactic activity of HXA<sub>3</sub>**

Hepoxilin A<sub>3</sub> caused strong chemotaxis of human neutrophils at concentrations as low as 30-40 nM (Fig. 26). The dose dependence of the chemotactic activity revealed biphasic behaviour in that it was attenuated at higher concentrations. Hepoxilin A<sub>3</sub>, up to 10  $\mu$ M, did not induce damage to cells as determined by the trypan blue exclusion test. The concentration of HXA<sub>3</sub> required to achieve the maximal chemotactic response is comparable with LTB<sub>4</sub>, however, the intensity of the chemotactic effect was higher for LTB<sub>4</sub>. Another 12-LOX pathway product, 12-HETE, did not exhibit any chemotactic activity in the concentration range tested. The HXA<sub>3</sub>-induced chemotaxis was completely abolished by the G-protein receptor inhibitor, pertussis toxin (2  $\mu$ g/ml; 90 min), while remaining unaffected by BSA (1 mg/ml).

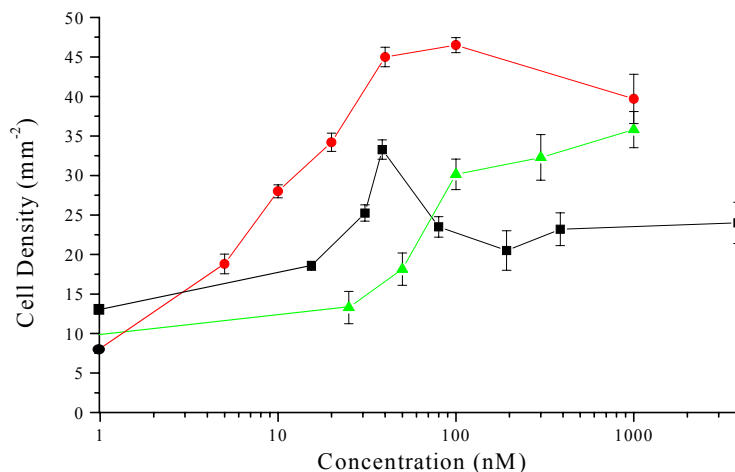


Figure 26. HXA<sub>3</sub> induced chemotaxis of human neutrophils. Chemotaxis by HXA<sub>3</sub> ■, LTB<sub>4</sub> ●, and fMLP ◆ was measured as described in Materials and Methods. Mean values  $\pm$  SE of six estimations using three different neutrophil preparations are given.

### **3.9 Calcium release**

Human neutrophils were isolated and pre-treated with Fura-2/AM as described in Materials and Methods. Changes in intracellular calcium were measured using a Fluorescence Spectrophotometer. Contrary to earlier reports, the addition of the free acid of HXA<sub>3</sub> (7  $\mu$ M) caused an immediate transient release of calcium which was equivalent to  $\sim$ 50% the extent produced by 100 nM fMLP (Fig. 27). The extent of the calcium signal was found to be dose-dependent in the range between 1 to 7  $\mu$ M. No signal was detected below 1  $\mu$ M. Following on this work, Reynaud *et al.* (1999) restudied the actions and found that the lack of biological

actions of the free acid was due to an artifact caused by the solvent DMSO.

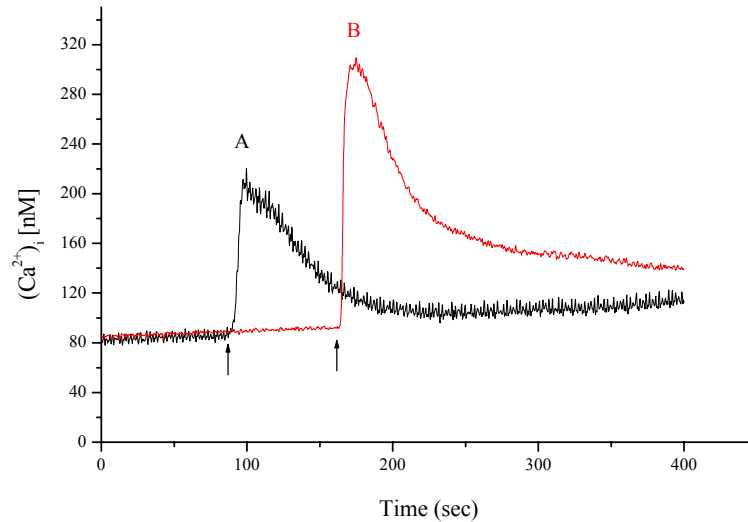


Figure 27. Calcium release in human neutrophils by the free acid of HXA<sub>3</sub> (7 μM; Trace A) and fMLP (0.1 μM; Trace B). The cells were loaded with Fura-2/AM and intracellular calcium measured as described in Materials and Methods. Arrows indicate time of addition of agonists. [Ca<sup>2+</sup>]<sub>i</sub>, intracellular free calcium.

The time profile produced by both HXA<sub>3</sub> and fMLP resemble each other in that they produce a rapid, instantaneous rise in calcium followed by a rapid return (~ 1 min) to the base line. The calcium chelator EGTA reduced but did not abolish the signal, thus excluding the contribution of an influx of extracellular calcium for the signal. The intracellular calcium pump inhibitor, thapsigargin (0.25 μM), abolished the signal.

### **3.10 Aggregatory activity of HXA<sub>3</sub>**

The aggregatory effect of HXA<sub>3</sub> on human neutrophils was measured using a Labor APACT aggregometer as described in Materials and Methods. HXA<sub>3</sub> did not elicit aggregation within the concentration range at which chemotaxis occurred. This suggests that the chemotactic effect of HXA<sub>3</sub> may be mechanistically different from that exerted by fMLP and more specific. The effect of HXA<sub>3</sub> on fMLP induced aggregation was also investigated. Hepoxilin, within the concentration range that induced chemotaxis, inhibited fMLP-induced aggregation (Fig. 28).

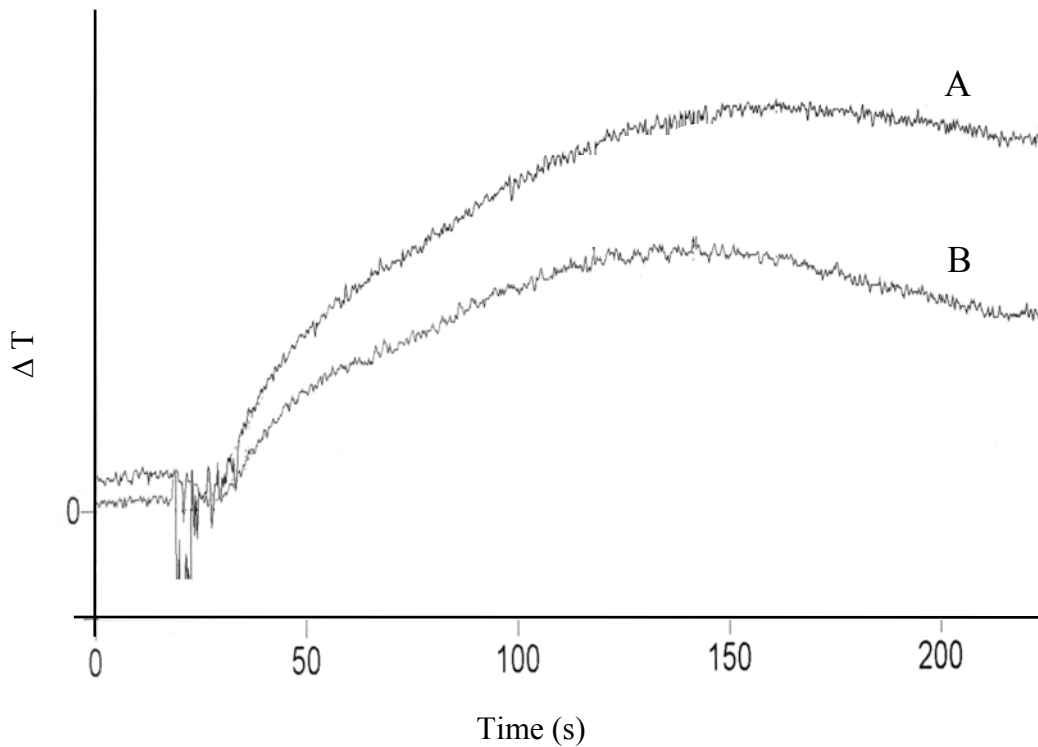


Figure 28. Effect of HXA<sub>3</sub> on fMLP induced aggregation. Human neutrophils ( $5 \times 10^6/\text{ml}$ ) were stimulated with 100 nM fMLP in the absence (A) or presence (B) of 100 nM HXA<sub>3</sub> and the change in transmission ( $\Delta T$ ) measured as described in Materials and Methods. A representative trace from 5 independent experiments ( $d=2$ ) is shown.

The dose dependent effect of HXA<sub>3</sub> on fMLP induced aggregation revealed biphasic behaviour (Table 11). The inhibitory effect observed at low HXA<sub>3</sub> concentrations (30 –100 nM) was attenuated at higher concentrations. The inhibitory effect of 100 nM HXA<sub>3</sub> was found to be statistically significant at the  $P<0.005$  level.

Table 11. Effect of HXA<sub>3</sub> on fMLP induced neutrophil aggregation. The cells were preincubated in the presence of various concentrations of HXA<sub>3</sub> for 15 s before the addition of fMLP. For further experimental details see Fig. 28. Results are expressed as maximum % transmission.

	Mean	Standard error	Determinations
fMLP	10.55	0.47	10
10 nM HXA <sub>3</sub> + fMLP	8.64	0.46	5
30 nM HXA <sub>3</sub> + fMLP	8.32	0.78	5
100 nM HXA <sub>3</sub> + fMLP	6.89	0.75	10
300 nM HXA <sub>3</sub> + fMLP	8.8	-	2
1000 nM HXA <sub>3</sub> + fMLP	10.15	-	2

The effect of HXA<sub>3</sub> on neutrophil-endothelial cell adhesion was also investigated as it has been suggested to be important in pathophysiology. The bovine endothelial cell line GM-7373 was grown to 100% confluence in 0.1% gelatine coated 24 well plates. <sup>14</sup>C-arachidonic acid labelled human neutrophils were added in the absence and presence of various concentrations of HXA<sub>3</sub>. No significant adhesion was detected.

### **3.11 cAMP release**

The effect of HXA<sub>3</sub> on cAMP release and fMLP induced cAMP release was measured by ELISA according to the manufacturers recommendations. Three concentrations of HXA<sub>3</sub> were tested (10, 100 and 1000 nM). The lower two concentrations had no effect on cAMP release whereas 1000 nM resulted in a 2-3 fold increase in cAMP levels as compared to the basal level of release. This may be due to the calcium release which occurs at this concentration.

The dose dependence of the effect of HXA<sub>3</sub> on fMLP induced cAMP levels resembles the chemotactic and aggregatory effects in that a biphasic concentration effect was observed (Fig. 29). Hepoxilin A<sub>3</sub> (100 nM) resulted in a 2-3 fold increase in fMLP induced cAMP levels whereas this effect was attenuated at 1000 nM.

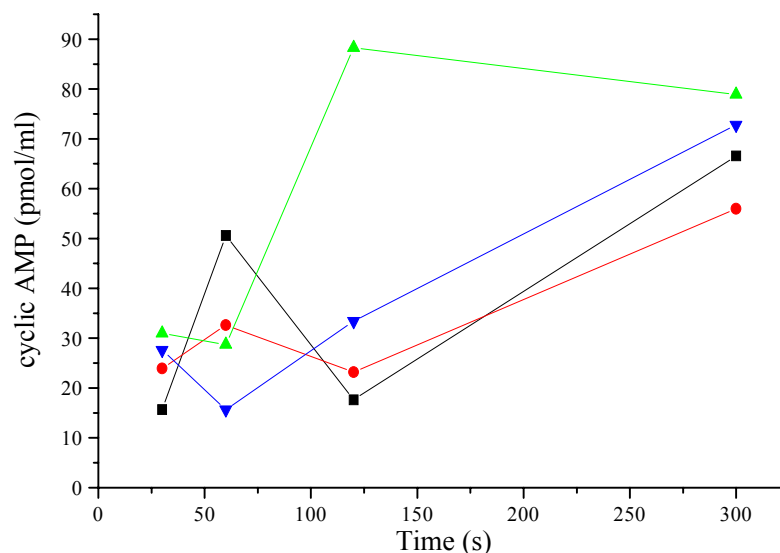


Figure 29. Effect of HXA<sub>3</sub> on fMLP induced cAMP levels in human neutrophils. (fMLP ■, 10 nM HXA<sub>3</sub> + fMLP ●, 100 nM HXA<sub>3</sub> + fMLP ▲ and 1000 nM HXA<sub>3</sub> + fMLP ▼). Graph is representative of two different neutrophil preparations from different donors (d = 4).

### **3.12 Arachidonic acid release and Leukotriene B<sub>4</sub> formation**

As it has earlier been shown that the methyl ester of HXA<sub>3</sub> causes release of arachidonic acid and that the free acid causes release of calcium from intracellular stores at higher concentrations, the free acid was expected to activate phospholipases with a concomitant liberation of arachidonic acid. Contrary to this expectation, HXA<sub>3</sub> in a concentration range between 1 and 5  $\mu$ M caused only a slight insignificant release of AA as compared to the control without agonist. Under identical conditions a strong effect by 100 nM fMLP was observed. This difference in response may in part be due to the differences in intensity of the calcium signals; it could also suggest that the appearance of a calcium signal is not sufficient for the activation of phospholipases.

When the neutrophils were pre-treated with varying concentrations of HXA<sub>3</sub> for 5 min, a dose-dependent modulation of the fMLP-induced liberation of AA was observed as measured 5 min following the addition of fMLP (Table 12).

Table 12. Submicromolar concentrations of HXA<sub>3</sub> blunt the fMLP-induced arachidonic acid release in human neutrophils. Arachidonic acid release was determined using cells prelabelled with [1-<sup>14</sup>C] arachidonic acid, the lipids extracted, separated by TLC and radioactivity determined. Number of experiments using different neutrophil preparations is indicated in parenthesis.

HXA <sub>3</sub> (nM)	AA Release (% of vehicle control)
0	339 ± 13 (6)
40	307 ± 15 (5)
100	278 ± 16* (6)
1000	318 ± 7 (5)

\* denotes significance against the control according to student's *t*-test ( $P < 0.02$ ).

At a concentration of 100 nM HXA<sub>3</sub>, the effect of 100 nM fMLP was significantly blunted. This blunting effect, however, disappeared at higher concentrations as for the aggregatory action. At concentrations higher than 1 μM, HXA<sub>3</sub> induced a slight increase in the fMLP-induced AA liberation. The priming effect of 1 μM HXA<sub>3</sub> was however not statistically significant.

In cells not pre-treated with HXA<sub>3</sub>, there was a lag period of about 15 s in the liberation of AA (Fig. 30) which was abolished by pre-treatment with 1 μM HXA<sub>3</sub>. The fMLP-induced AA liberation in HXA<sub>3</sub> primed cells was partially inhibited by the β-blocker propranolol, which is known to inhibit the phospholipase D (PLD) pathway and phosphatidic acid phosphohydrolase activity. This suggests the involvement of the PLD pathway in this process, which is in agreement with earlier work using the methyl ester.

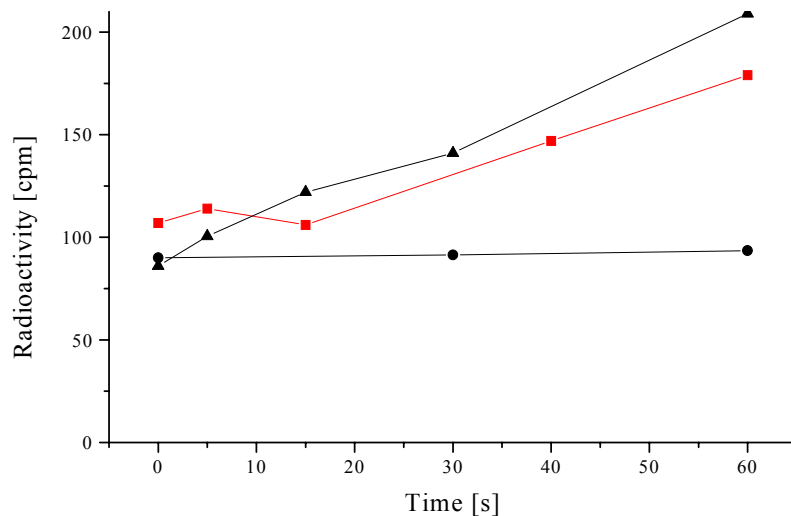


Figure 30. Effect of the free acid of HXA<sub>3</sub> on the initial phase of fMLP-induced arachidonic acid release. Prelabelled [1-<sup>14</sup>C] arachidonic acid neutrophils (●) were stimulated with 100 nM fMLP in the absence (■) or presence of 1 μM HXA<sub>3</sub> (▲). Plot is representative of 5 independent experiments that revealed consistent time profiles.

The arachidonic acid released following stimulation of the cells with 1 μM HXA<sub>3</sub> + 100 nM fMLP originated exclusively from the phospholipids and mainly from the phosphatidylethanolamine (PE) pool (Table 13), as judged by phospholipid remodelling experiments using 2-dimensional TLC as described in Materials and Methods.

Table 13. Effect of 1 μM HXA<sub>3</sub> on the phosphatidylethanolamine pool in [1-<sup>14</sup>C] arachidonic acid labelled neutrophils in the presence and absence of 100nM fMLP. Reaction was stopped, extracted and analysed by 2-dimensional TLC as described in Materials and Methods. Results expressed as mean CPM (n = 2, d = 4).

	phosphatidylethanolamine
Control	90.8
100 nM fMLP	63.6
1 μM HXA <sub>3</sub> + 100 nM fMLP	58.2*
1 μM HXA <sub>3</sub>	70.5

\*denotes significance against the control according to student's *t*-test ( $P < 0.05$ ).

Similar observations were also made for the formation of leukotriene B<sub>4</sub>. Hepoxilin A<sub>3</sub> caused only a very slight, if any, formation of LTB<sub>4</sub>, which was significantly higher following fMLP stimulation. Both fMLP and HXA<sub>3</sub> are poor releasers of LTB<sub>4</sub> in human neutrophils; therefore, the chemotactic activities can not be associated with the formation of this 5-LOX derived eicosanoid.

### **3.13 Respiratory burst**

Two independent methods were applied. The superoxide anion production by human neutrophils due to the reduction of ferricytochrome C was measured spectrophotometrically (550 nm) as described in Materials and Methods. Both fMLP (100 nM;  $V_{\max} = 64.42 \pm 9.6$  mOD/min, n=3) and PMA (100 nM;  $V_{\max} = 48.64 \pm 1.30$  mOD/min, n=3) caused an increase in superoxide anion production. HXA<sub>3</sub> up to 5  $\mu$ M had no effect. HXA<sub>3</sub> had no effect on the fMLP and PMA induced superoxide anion production.

Secondly, agonist-induced antimycin A-insensitive oxygen uptake was recorded at 37°C with an Oxygen Meter as described in Materials and Methods. Under these conditions, 100 nM fMLP caused a strong transient oxygen uptake ('respiratory burst') for 1-2 min (initial rate :  $3.5 \pm 0.3$  nmol/min). This was blocked by 100% by pre-treatment of the cells with the protein kinase C inhibitor staurosporine (1  $\mu$ M). Hepoxilin A<sub>3</sub>, at a concentration of 5  $\mu$ M, produced a small but insignificant oxygen uptake. No effect was observed using lower concentrations.

### **3.14 Regulatory volume decrease (RVD)**

It has been earlier reported (Margalit *et al.*, 1993) that the methyl ester of HXA<sub>3</sub> plays a role in RVD in human platelets. The role of the free acid in RVD in human neutrophils was therefore investigated. Human neutrophils were isolated as described under Materials and Methods, resuspended at a concentration of  $10 \times 10^6$  cells/ml and treated with 1  $\mu$ M HXA<sub>3</sub> for electron microscopic analysis and from 20 nM to 5  $\mu$ M for flow cytometry analysis. The effect of HXA<sub>3</sub> on RVD as determined using a fluorescence-activated cell sorter (FACS) was measured immediately after the addition of HXA<sub>3</sub> and after 5 min incubation (Table 14). The data failed to show any significant changes in cell volume within the concentration range tested.

Table 14. Effect of HXA<sub>3</sub> on regulatory volume decrease in human neutrophils as determined by flow-cytometry (n = 1, d =2).

HXA <sub>3</sub> Concentration	Mean FSC-Height (Time 0)	Mean FSC-Height (Time 5 min)
0	455.71	446.74
20 nM	467.47	468.41
100 nM	467.82	466.42
1 $\mu$ M	471.30	470.96
5 $\mu$ M	468.75	471.18

(FSC :- forward light scatter, reflects the distribution of the neutrophil size)